Control of Surgical Robots with Time Delay using Model Predictive Control

by

Jasmeet Singh Ladoiye

Thesis submitted
In partial fulfillment of the requirements
For the Master's in Applied Science degree in
Mechanical Engineering

uOttawa

Department of Mechanical Engineering
Faculty of Engineering

University of Ottawa

Abstract

Minimum invasive surgery is based on bilateral teleoperation in which surgeon interacts with the master side to the slave side that is located at a distance. The synchronization in between the two ends is through a communication channel. The primary objective in the telesurgery is the position and force tracking providing the surgeon with high fidelity. The presence of time delays in the communication channels makes the realization more difficult, and sometimes it may even destabilize the system.

The work focuses on a design of the force control system by using Model Predictive Control to compensate for the effects of the time delay related to the use of surgical arms. Another vital issue of minimum impact velocity during contact with the environment has been tried to achieve by using the prediction from the Model Predictive Control to prevent accidental tissue damage. This work also addresses a problem of the developing a simple delayed free predictive kinematic imaging to understand the type of behavior of the system during contact with the environment when no perception is available.

Dedication

This work is dedicated to my parents, and my loved ones without whose prayers, unmatchable hard work and support that wouldn't have been possible to pursue my dreams. Their constant and undoubted support for me which helped in this hard but beautiful journey of mine, and last but not the least my younger sister, Manjot Kaur, and my other cousins whose unabashed love for me, encourages me to achieve the goals.

Acknowledgments

This thesis has been very challenging and enjoyable journey. I would like to thank firstly the Faculty of Engineering, the University of Ottawa for giving me a chance to work on this topic.

I would like to express my deep gratitude to my supervisor's Dr. Dan Necsulescu and Dr. Jurek Sasiadek who saw the capability in me and took me under his supervision and guided me through this tough journey. Their sage advice, support and patient encouragement made it possible for me to finish this work. Their reviews and inputs always helped me improve different aspects of this thesis.

Also, I would like to thank all my colleagues in the lab Arpit Ainchwar, Mohit Sain, Alireza Mirghesani, Vishal Koppula, Aliakbar Baadliwala and Hamid Reza Fallah whose ideas, help, and support played a big part in the completion of this thesis.

I would also like to thank my friends Piyush Katyal, Chandan Kalra, Abhimanyu Singh Beniwal, Emilcen Hamilton and Vivan Luthi Yang who stood with me and supported me in this journey.

A sincere thanks to Khushi Soi and Harshee Soi for diligent proofreading of this thesis.

Most importantly I would like to thank my parents who were always pateint and believed in me and supported my every decision, The Creator who made everything possible for me to achieve and gave me strength, courage, and guidance to go through this phase of my life.

Table of Contents

List of Figures

List of Tables

Abbreviations

1. MIRS – Minimally Invasive Robotic Surgery
2. MIS - Minimally invasive surgery
3. MPC – Model Predictive Controller
4. OR – Operating room
5. CT – Computer tomography
6. MRI- Magnet Resonance Imaging
7. PID- Proportional-Integral-Derivative
8. LQR- Linear Quadratic Regulator
9. QP – Quadratic Program
10. PI – Proportional-Integral
11. 3D - three Dimensional
12. 2D – two Dimensional
13. ARTEMIS - Advanced Robot and Telemanipulation System for Minimal Invasive Surgery.

Chapter 1
Introduction

This research thesis outlines the Minimum Invasive Robotic Surgery (MIRS), a rapidly expanding technology in the field of medical robotics. This thesis explores the teleoperated MIRS systems basic control structure along with a solution to the force feedback for the systems with time delay compensations giving the surgical systems an extra dimension. It gives us a brief study of the abilities of how Model Predictive Controller (MPC) can be used to enhance the abilities of a system in comparison to the Proportional-Integral-Derivative (PID) controller.

1.1. Evolution of Surgery

In the past few decades, with the advancement in the technology in the methods of carrying out surgeries, there is a huge paradigm shift for the health institutions and patients. New robotic telesurgical techniques have evolved from the traditional open surgery methods as shown in Figure 1. Open surgery is the kind of surgery that involves direct physical contact of the surgeon with the patient providing the surgeon the greatest visual and tactile information of the tissue operated on. Advanced surgical techniques use Minimally Invasive Surgery (MIS) tools to carry out the surgery through the tiny orifices on the human body.

Open surgery provides surgeons an unobstructed three-dimensional (3D) view of the environment with the ability to feel the tissues. It also is a useful procedure such that the surgeon can use its natural hand's dexterity to carry out the operation with accessibility to the widest possible instruments [1]. However, the patient is subjected to the significant pain and inflammation due to the large incisions on the body.

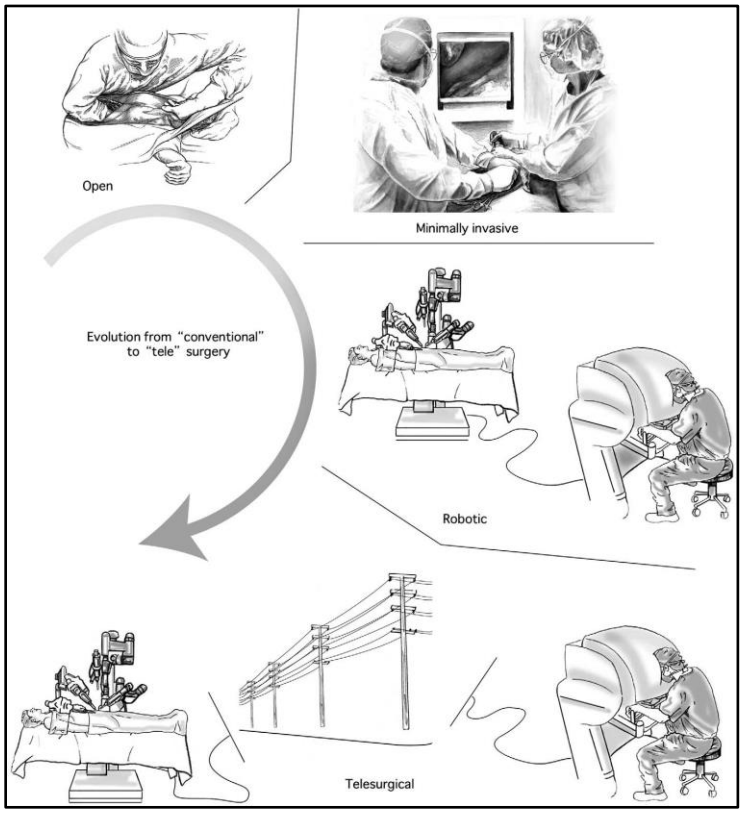

FIGURE 1: EVOLUTION FROM 'TRADITIONAL' TO 'TELE' SURGERY [1]

Minimally invasive surgery (MIS) is a technique to carry out operation brought out in the midst of the 20th century. The surgeon operates through tiny incisions of about 1 cm made on the patient's body by using specially designed surgical tools as shown in Figure 2.This technique holds patient side benefits over traditional open surgery such as decreased pain, reduced surgical trauma on the tissues, and a short stay at the hospitals. Since the surgery operates through tiny incisions that

offer cosmetic benefits to the patients because of smaller visible scars as compared to open surgery. MIS benefits patients but also have some demerits for the surgeon as described by Huang et al. [2], Sauerland et al. [3] among others. Tissues properties such as stiffness are not assessable to the surgeon due to lack of direct manual contact with the patient's body. Moreover, direct hand to eye coordination, dexterity inside the patient's body loses as compared to the open surgery. The long instruments in MIS processes operate through a fixed incision on the human body that suffers the loss of two degrees of freedom. A surgeon requires intensive training to carryout MIS. It is time-consuming as compared to traditional techniques making simple tasks such as tying knot time-consuming. Today, surgical procedures such as removal of the appendix (appendectomy), hernia repair, gallbladder removal (cholecystectomy) and gastro-oesophageal reflux disease are carried out using MIS techniques. MIS is not recommended for the complex processes especially cardiac surgery as explained by Wullstein et al.[4].

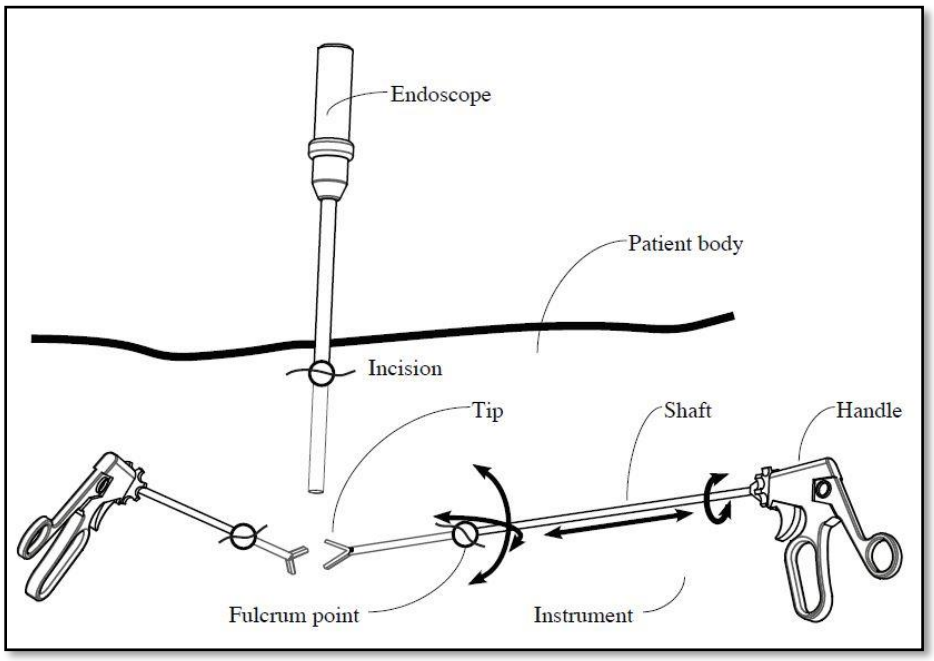

FIGURE 2: A VIEW OF THE OPERATION SITE PROVIDED BY THE ENDOSCOPIC CAMERA [5]

To overcome the limitations of the MIS, minimally invasive robotic surgery (MIRS) plays a vital role. In this system, the instruments are not directly handled by the surgeon at the operating room (OR) but are remotely commanded by the surgeon while working at the input console and devices are fitted onto the distant robot. The robot at the patient end works on the inputs provided by the surgeon operating from the master end. Advanced MIRS system with the ability to perform surgery remotely comprises three main components:

1. Slave
2. Master
3. The communication link between slave and master.

The slave system comprises several subsystems: The minimum invasive instruments should at least have 2 DOF's to guarantee full manipulability inside the body and should allow measurements of the environment. The visual feedback to the surgeon helps him to make the decision making as per the situation. More intelligent control laws can be developed by using the sensory data from the salve end. Force measurement will help to limit the maximum manipulation force on the tissues. Moreover, it can also help to compensate for the organ movement during the operation that will prevent the damage to the muscles. MIRS tools must be lightweight, such that during the time of changeover of the tools one person can easily handle them. This is very crucial especially during emergency situations when direct access to the patient is required. Hence, lightweight instruments also reduce the set-up time before surgery.

The master system provides inputs to the slave robot in the form of position or force trajectories. The perception of the slave end is received at the master end through 3D vision as per which surgeon does the decision making. High-quality feedback in the form of tactile and kinesthetic feedback must be provided at the master end. Tactile feedback is necessary to get a sense of palpation from the body, as in open surgery. Hence it is essential to increase the quality of operation [6]. To improve more accuracy of the MIRS, scaling of the surgeon's motion along with the tremor filtering are additional features added at the master end. Augmented reality is provided by the high definition cameras that help to get details of the environment where one is operating at.

The communication system is responsible for setting up a link between the master and the slave robot. It must be flexible enough such that to allow the connection of different master stations when more than one surgeons are needed or for training purposes. Another advantage of having a flexible system is in the emergency when an inexperienced surgeon needs help from an experienced surgeon in between the surgery. The desired communication system should be safe and secure with guaranteed bandwidth and no undesirable third-party listening. Network systems also suffer from communication delays that also happens because of many other reasons.

Faster surgery helps in two different ways: costs has to be reduced since the present systems are slow and will also reduce the postoperative complications for the patient. By these efforts, MIRS systems will get safer and more rapid in the future.

1.2. Motivation

We use our hands in day to day life from simple to complex tasks. During the initial learning phase too, surgeons learn to use their hand's ability to accomplish delicate tasks. They act as receptors through which they assess the health of a tissue. MIS is a step backward when we compare it with traditional open surgery apart from having patients side advantages such as reduced risk of infection, faster recovery and smaller scars. Since haptic perception is not available, MIS reduces the surgeon's dexterity that's why surgeons have to go through rigorous training to learn and adapt to compensate for the loss of the sense of touch.

MIRS systems should ideally preserve the advantages of the MIS for the patient but should also overcome the limitations offered by the MIS, i.e. restricting the skills of the surgeon. The MIRS system should provide a "Virtual Open Surgery" environment performed in the minimum invasive way. Computers enhanced dexterity, 3D vision quality and sense of touch is responsible for ensuring open surgery environment to the surgeon.

Today's commercially available MIRS systems restore hand-eye coordination, also preserves and extends the dexterity of surgeons hand, and precision of the input given by the surgeon is increased through motion scaling and tremor filtering. They lack in providing full forced feedback to the surgeon, and they still have to rely solely on the visual feedback from the patient's end.

Another major problem in the teleoperated systems is due to network systems, caused by the long-distance or wireless links [7],[8]. Bandwidth limitation packets losses, sampling, and delays belong more precisely to this problem that poses another challenge to telerobotic surgery. The solution to the time delays and packet loss compensation in network systems is discussed in [9] by using Model Predictive Controller.

Research in the field of augmented reality is making the vision of "virtual open surgery." closer to reality. Traditionally, CT (computed tomography), and MRI (magnet resonance imaging) scan in the form of 2D data is presented over the OR wall on the lightbox that helps the surgeon to look up and mentally reorient the image to match the operating site. The 3D vision helps us to provide the same information directly in the same field of view of the surgeon, aligned directly with the working area. Hence augmented reality improves the capabilities of the surgeon by sharing the information that is inaccessible to the human senses.

1.3. Objectives

The prime objective of this work is to develop novel control structure capable of providing force feedback to the surgeon in a surgical robot capable of minimally invasive robotic surgery (MIRS). The impact of the tool while contacting the body has been tried to minimize by using Model Predictive Controller (MPC), that will provide enhanced dexterity compared to conventional techniques of control. The final novelty aims at delivering kinematic predictive imaging that will

provide the surgeon delayed free perception of the robot for the time when no perception is available to the surgeon for a current instant of time.

1.4. Thesis formation

The thesis consists of 8 chapters that will walk through the reader through the different stages of works related to the development of the control of the MIRS. The thesis mainly focusses on developing the control framework of a MIRS, primarily focusing on the development of the force feedback of the system.

Chapter 2 provides us with the literature review of the previous work carried out related to the field. This chapter begins by discussing the evolution of the open surgery to the minimum invasive robotic surgery. It also explains the advantages of having haptic feedback, with the importance of the impact model and kinematic predictive imaging in a surgical arm.

Chapter 3 discusses the control theory of predictive model control. It explains the control laws of the MPC with the literature of MPC to control time-delayed systems. It also consists of a section that compares MPC with the PID controller.

Chapter 4 begins with a discussion of the control techniques available for the force control and moves on to control algorithms of the force control with MPC formulation for the time delayed system.

Chapter 5 outlines a system that is modeled to carry out the simulation work. Firstly, they discuss the force control architecture and its various components at master and slave ends. Lastly, they look into the kinematic imaging control scheme to end with the chapter.

Chapter 6 detailed about the simulation results along with discussions, including various graphs to explain the novelty of the work.

Chapter 7 and 8 concludes the thesis by discussing the work in a nutshell and conclusion drawn and finish with the recommendation for future work.

Chapter 2
Literature Review

An excellent and reliable MIRS system should have following features from the surgeon's point of view [10]: Advanced MIRS system should provide us kinesthetic and haptic feedback, that will provide the surgeon with a perception of the tissues and underlying structures. Cartesian control along with the visual 3D feedback should give a right hand to eye coordination like traditional open surgery. Intelligent assistance function such as grasping, automatic positioning, cutting along with safety features is also much desirable. The actuated minimum invasive tools are expected to provide high precision and full manipulability inside the body.

Presently several research organizations at international research institutes and companies are working towards the development of the MIRS systems. The robotic medical systems are classified into two types: Assistance systems and complete MIRS telepresence systems, containing master and slave subsystems.

Robotic assistance systems act as flexible and intelligent tool holders [11] or mainly used to hold the laparoscope [12] [13] [14]. Surgeon's interaction with the assistance systems is either via voice [12] [13] or through force sensor mounted on the robot [11]. The assistance systems cannot achieve all the benefits of the complete MIRS system.

This chapter discusses the telepresence systems developed at different international research centers and companies. After that, the chapter presents the importance of haptic feedback in the robotic systems in detail.

2.1. MIRS Systems in Research Organizations

This part of the chapter gives us an overview of the various MIRS systems developed so far across the research organizations throughout the world.

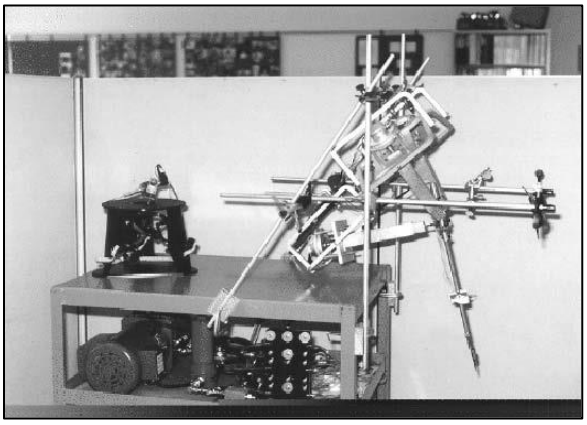

FIGURE 3: MASTER (LEFT) AND SLAVE (RIGHT) [15]

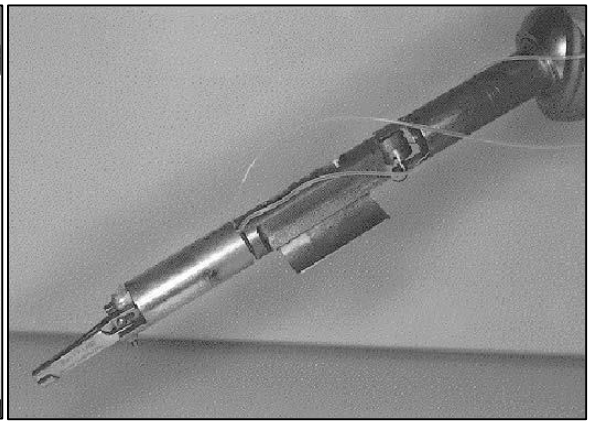

FIGURE 4: MILLIROBOT [15]

Researchers at UC Berkeley / UC San Francisco developed a telesurgical system [15] as described in the Figures 3 and 4. The slave end of the robot is based on the Millirobot^{TM} with a diameter of 10mm, that has six DoFs with two actuated DoFs inside the body, Hence providing full manipulability.

The first-generation master side was based on the Impulse Engine™ from the Immersion Inc. Later, the master end was replaced with the PHANToM and slave end with the modified Millirobot. No force feedback is available in both the versions of the telesurgical arm.

An arm with the ability to provide six DoF force/torque feedback was developed at KAIST [16] [17] in Korea for the microsurgical tasks. This model used a modified industrial robot for carrying out the micromanipulation. However, the industrial arm was not designed for use in the operating room (OR). Moreover, the system lacked in manipulability if used for laparoscopic surgery.

Another arm named ARTEMIS (Advanced Robot and Telemanipulation System for Minimal Invasive Surgery) was developed at "Forschungs-Zentrum Karlsruhe" in Germany [18]. The slave arm consists of two-three arms, out of which two are used to hold and manipulate instruments while others keep the laparoscope. As a drawback, this arm does not have force feedback, and a slave end lacks with the additional degrees of freedom.

2.2. Commercially available MIRS Systems

MIRS systems for clinical use are primarily dominated by two robotic systems named as: The Zeus® system by Computer Motion [19] and the daVinci® Arm by Intuitive Surgical® [20]. The Zeus® arm was available until 2003 when the Intuitive Surgical acquired the Computer Motion after time taking the battle for a patent. Zeus® arm consists of a surgeon's console and three

individual robotic arms mounted on the operating table. The middle arm handles the laparoscopic camera that can either be controlled through voice or manually through a pin pad. The other two arms were used to guide various minimum invasive instruments. The input console of the system closely recreated the kinematics of conventional minimally invasive surgery, simulating the restricted movements about the point of incision. The surgeons trained in traditional MIS can adapt to this system and operate this system efficiently.

Currently, the daVinci® system by Intuitive Surgical® is the most widely used commercial system as shown in Figure 5 [20]. It contains three main components: a master console with a three-dimensional video display, a robotic manipulator with four arms and a vision cart. The three-dimensional vision is possible using two separate optic channels in the stereo laparoscopy. The three-dimensional image of the operative site is displayed at the surgeon's screen through the stereo display. The laparoscopic camera is controlled by the surgeon using a combination of hand and foot controls.

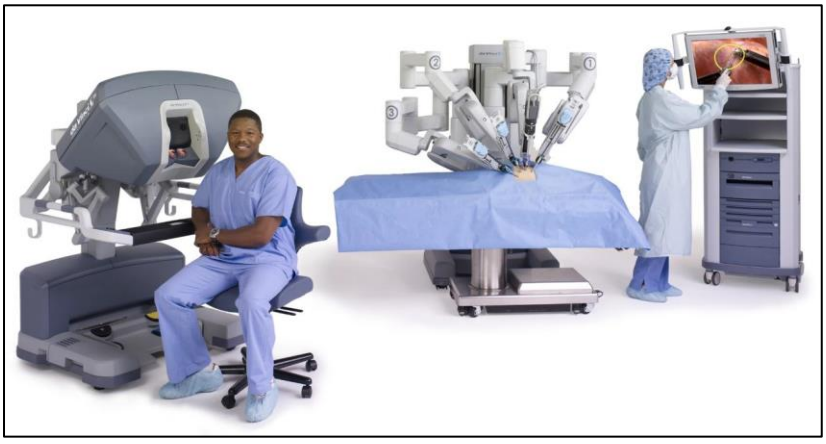

FIGURE 5: INTUITIVE SURGICAL DA VINCI SURGICAL ARM [20]

Following the daVinci®'s success, a variety of research efforts being performed to develop new MIRS systems. A second-generation robotic arm (MIRO) was developed by German Aerospace Center (DLR) that is to be used in MicroSurge robotic system [21]. The arm weights less than 10 kg, and the arm can be attached directly to the operating table, unlike DaVinci arm.

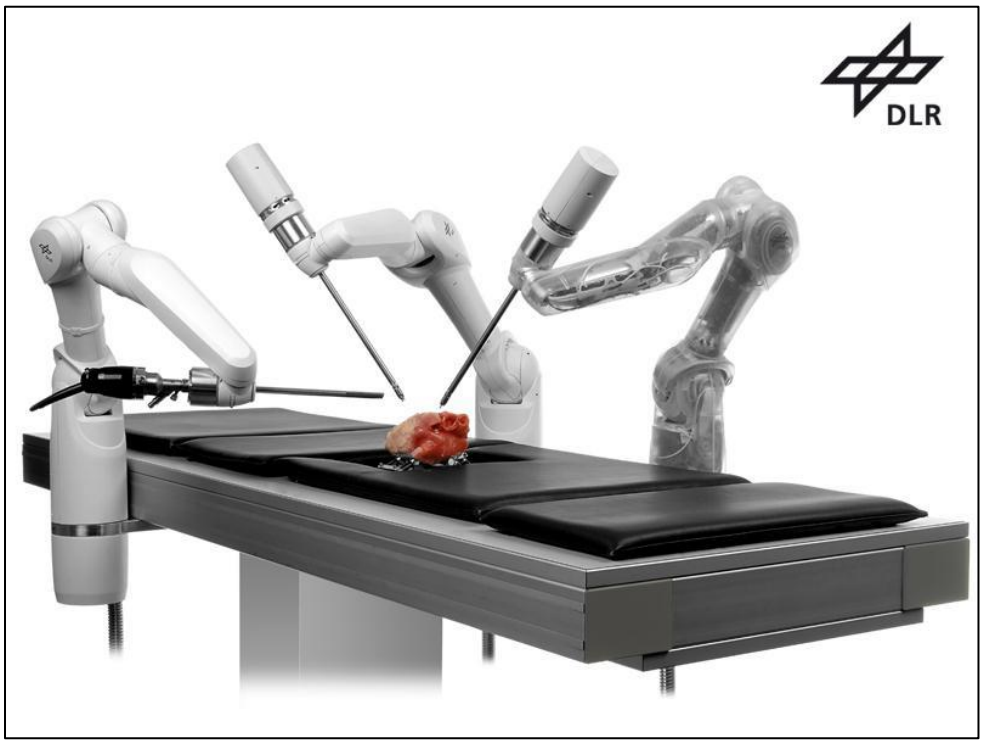

FIGURE 6: GERMAN AEROSPACE CENTERS MICROSURGE SYSTEM [21] [22]

The MicroSurge system consists of 3 MIRO arms each having 7 DoF: two of them using laparoscopic tools and the third arm holds the endoscopic camera [22] as shown in Figure 6.

SOFIE® (Surgeon's Operating Force-feedback Interface Eindhoven) robotic arm was developed by the researchers at the Technical University of Eindhoven to improve the force feedback of the existing da Vinci system [23] as shown in Figure 7. SOFIE® was designed with the following

design specifications by keeping the following things in mind: improved dexterity by adding additional DOFs at the instrument tip to improve organ approach; much easier setup for the operation; reduced system size and reduced costs; and forced feedback for the surgeon that will reduce the operating time and will improve the patients safety.

FIGURE 7: SOFIE® ROBOT [23]

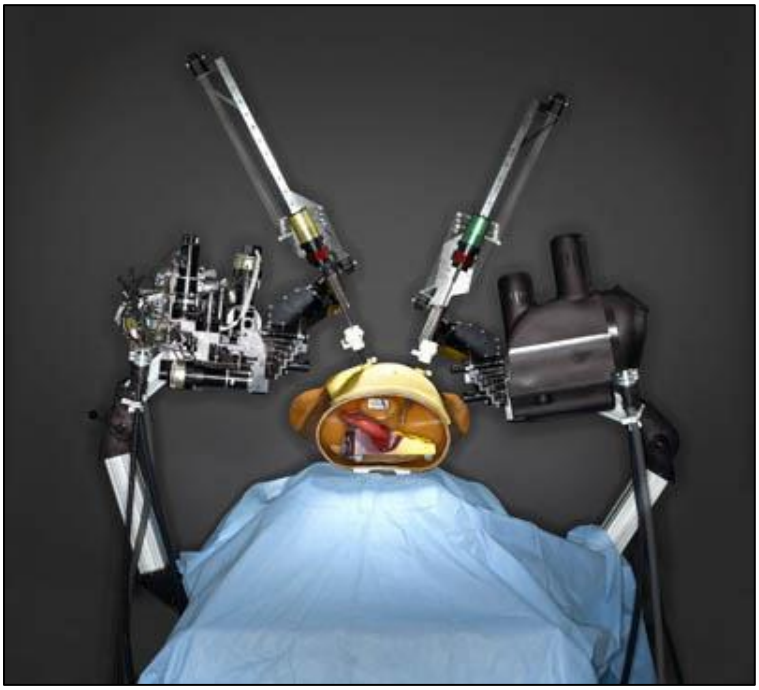

FIGURE 8: RAVEN®'S TELESURGICAL SYSTEM [24]

The BioRobotics Lab at the University of Washington developed a robot named RAVEN® that can carry out telerobotic surgery [24] as shown in Figure 8. The robot aimed at researching the effects of distances on the latency. The RAVEN® is using Sensible PHANTOM® Omni controllers to carry out the telerobotic surgeries and is not capable of providing haptic feedback to the surgeon.

2.3. Autonomy in MIRS systems

The advanced telesurgical systems are incorporated with some sensors that provide multi-sensory information to the surgeon. The data is processed by the surgeon that helps him to drive the robot. Processing of multisensory data offered to the surgeons lead to high demand for sensomotoric skills, that is hard to meet. To reduce these strong demands, new control strategies were developed that shares the control between the surgeon and the robot. Under the supervision of the surgeon, the robot takes the control over the tasks requiring high bandwidth, whereas the surgeon controls the functions of the master robot with low bandwidth.

One of the examples is the movement of the tool tip along the predefined path: the surgeon only commands the velocity (one DoF) whereas the robot is taking control of (six DoF).

The ROBODOC® system uses ORTHODOC® that helps in the preoperative planning of the motions that are required for the precise milling [42]. Preoperative CT images are uploaded to the ORTHODOC® system which creates a surgical plan. The ACROBOT® is used in the orthopedic

surgery, constrains the movement of the cutting tool based on the constraints applied to the preoperative planning phase [42]. Raven II system developed at the University of Washington can automate the tasks such as tremor ablation [43] and debridement [44].

In minimum invasive beating heart surgery, the position of the target is calculated in real time because of the position of the target change with the respiration and beating heart. It is a very crucial feature that is desired in the beating heart surgery. The robot compensates the hearts motion, such that the relative pose between the heart surface and the center of the tool remain the same. So, the surgeon is operating on a virtually stable heart as he was used to in on-pump surgery.

2.4. Telesurgery

Telecommunication revolution made the telerobotic surgery possible extending the reach of medical centers to the remote localities. On 7th September 2001, J.Marescaux with his team from European Institute of Tele-Surgery performed first transatlantic telerobotic surgery between Strasbourg, France, and New York, U.S.A by using Zeus® robot (By Computer Motion, Inc., Goleta, CA; now operated by Intuitive Surgical, Inc., Sunnyvale, CA) [45]. Based on the [46] it was estimated that it's relatively safe to perform the surgery if the time delay is less than 330ms. However, it becomes difficult for the operator to control the Zeus if the time delay exceeds 700ms. A high-quality Asynchronous Transfer Mode (ATM) fiber optic link was used to carry out the research. The optic link was providing not only the control signals and visual feedback but also serving connection for two-way video conferencing. The average lag of about 155 ms was

observed, out of which 85 ms lag was due to lag in transmission and 70 ms for coding and decoding of video signals.

M. Anvari carried out advanced laparoscopic surgery using the same robot at Center for Minimum Access Surgery (CMAS)/ McMaster University, Hamilton, Ontario on patients in the rural areas of Canada using Zeus robot in the year 2005 [47]. The average lag of about 150ms was observed using commercial high-speed link Virtual Private Network (VPN) protocol.

In 2006 a remotely controlled catheter guiding device guided by a robot was used to carry out heart ablation automatically, initiated and carried out by a team of doctors from Boston, MA [48]. A pre-operative CT scan of the patient with real-time electromagnetic navigation was used to direct the catheter to the desired location.

A remote surgery was conducted between Japan and Thailand in 2007, on a pig using the minimum invasive surgical system. It was observed that the UDP/IP protocol is safe to carry out the process, but packets loss was observed during the experiment. The round-trip data delay of about 124.7 ms was seen whereas average visual delay using low latency CODEC system was 540 ms [49].

Smith and Chauhan in 2012 [50] used daVinci® Simulator to carried out a study within the state of Florida to study the effects of distance on the latency. The simulator was set up with the delays of the real-time scenarios. Following observations were made in the study:

1. The surgeons could not detect the lag time till 200ms.
2. From 300ms to 500ms, they could detect the lag time, but they were able to compensate for it by pausing their movements.
3. However, after 600ms it becomes insecure as the settling time increases for the system as shown in Table 1.

TABLE 2.1:: *OBSERVATIONS OF THE DA VINCI SIMULATOR*

Time lag (milliseconds)	Effect on the system
0 – 200	Safe
200-500	Physically dependent on the surgeon
600 - more	Unsafe

The experimental data recorded [51] shows the randomness of the time delay and data losses when sending data through the internet. We have assumed deterministic time delays in each set of the three intervals to study the effectiveness of our proposed study which is needed to be relaxed in future.

2.5. Essential Components in Telesurgery

The ideal telesurgical system contains the following necessary elements that make a telesurgical team. A telesurgical team comprises Surgical robots, telecommunication equipment, surgeons and technical expertise, a patient with unmet needs and financial support as shown in Figure 9.

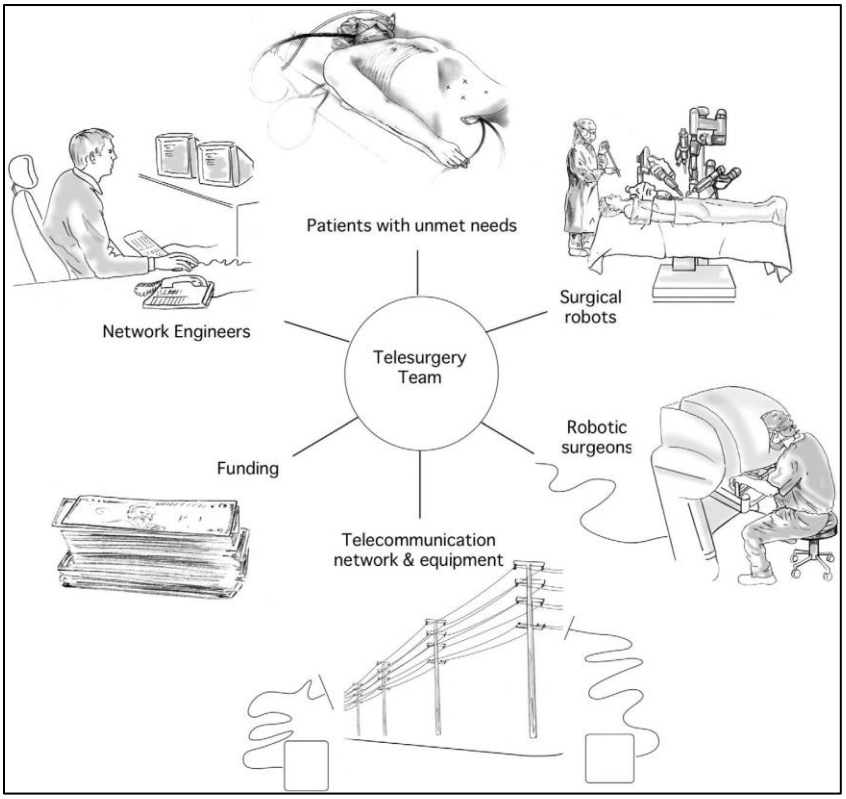

FIGURE 9: ESSENTIAL COMPONENTS IN TELESURGERY [1]

An ideal telesurgical network should have high bandwidth and low latency. A clear two-way reliable communication between local and remote sites is required to carry out a safe telerobotic surgery. Audio signals can be integrated into the same visual and robotic data signals by using a Voice Over Internet Protocol (VOIP) but a standard parallel voice-only connection can be used if the telesurgery network is limited. Two-way video conferencing in between master and slave end can also be used to enhance the practice of telesurgery. Lastly, and indeed the most important the telesurgery circuit needs a laparoscopic visualization of the operative field on the local and site end as shown in Figure 10.

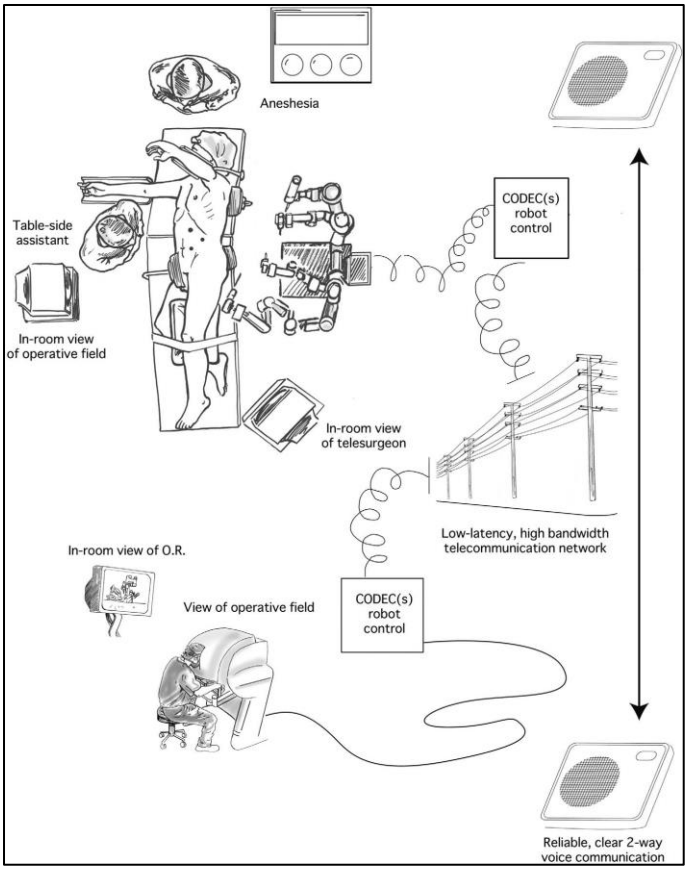

Figure 9: Essential components in telesurgery [1]

2.6. Delays in Telesurgery, Barriers, and Limitations

The prime objective of the telerobotic surgery is to mimic the normal process of operation at a distant place. The time delay in the process directly impacts the surgeon's performance, and the success of the operation under its effect largely depends on how effectively it can duplicate their onsite activities.

The time delay can be described as the control latency in the input from the surgeon's end to the patient end. Control latency can be defined as the time when the remote surgeon moves to the time when the surgical tool runs on the patient side. The system can cause control delay due to the following factors:

1. Delay in the electromechanical conversion of the signals from one form to another.
2. Time latency to send the digital signals from the master end to the patient's end.
3. Time is taken in the conversion of the mechanoelectrical conversion of joystick movements into digital signals.

The visual discrepancy is the other kind of delay in the network in the signal from patient to surgeon. Visual delay can be defined as the time from when an object moves in the operational field to when the surgeon sees the visual of the movement in control. Optical delay can be summed up related to three factors:

1. Compression and digital conversion from the laparoscopic camera by a video CODEC.
2. Transmission delay to transmit the video through the network.
3. Decompression of the transmitted video signal by remote CODEC for the display console.

The total time delay, i.e., efferent and the afferent delay between the surgeon and patient is known as Round-trip delay. Functionally, round-trip delay represents a time when the surgeon moves controller at the remote location to when such move is visible to the surgeon through vision at the

master console. The efficiency of CODECs and speed of transmission across the telecommunication network are the most contributing factors that affect the round time delay.

2.7. Impact of Haptic Feedback

The sensation of touch relies on some receptors such as mechanoreceptors and thermoreceptors. Mechanoreceptors are present in the muscles, tendons, and joints whereas thermoreceptors are embedded in the skin. The surface texture mostly characterized by the roughness that is related to the cutaneous system. The kinesthetic system deals with the weight of the object; it is the resistance of the object to rotational forces generated by limbs. The deformity of an object under the external force is related to the compliance domain. Objects having a scale less than fingertip comes under cutaneous area whereas larger objects are having weight are considered in the kinesthetic domain.

The terms force feedback, tactile feedback, and haptic feedback are generally used interchangeably in many of the studies. Haptic feedback is considered related to kinesthetic mechanoreceptors, and tactile feedback comes under the cutaneous domain. Both the fields require different physical sensors and displays. The measure of the cutting, suturing, etc. using multi-DOF force-torque sensors, and active measuring of the stiffness of the tissue comes under the force sensing. Tactile sensing uses the pressure sensitive sensors to resolve the force distribution problem.

This first contribution in this thesis is related to the development of the force feedback system in a surgical system suffering from time delays. The time delays have been considered deterministic to carry out the study that has to be relaxed in future work. To compensate for the time delay and its effects two approaches are described.

In open surgery, surgeons depend strongly on the sense of touch to determine the properties of the tissue during the operation. Haptic feedback gives them the sense of information about the health of the tissue and locates specific structures such as blood vessels or tumors. With the discovery of the MIS techniques, surgeons lost the access to the tissues that lost much of the haptic feedback from the operation site. Bholat et al. [25] concluded that haptic information from the operation site is still available in MIS and surgeon can even determine the size, shape, and compliance of the objects. But with the decrease in the structure sizes, it became more difficult. The forces applied during the operation varies from 0.3 N for bypass grafting [26] too few newtons during the tissue manipulation [27] [28] [29] [30] [31]. In the MIRS systems, the sense of haptic feedback gets lost since there is no direct contact between the surgeon's hand and tooltip.

With the experience in the robotic surgery, surgeons through expertise can interpret through the 3D vision the information related to the tissue deformation. However, this information varies from patients to patients and depends upon their health, tissue type, etc. [32]. Stiffer tissues such as bones, suture materials show no deformation at all. Therefore, the optimal and reliable tightness of the knot is difficult to guarantee [33]. Kitagawa et al. and Akinbiyi [34] [40] modified the existing EndoWrist® instrument fitted with 2 DoF strain gauges attached to the end of the effector.

The revised system displays the effective knot tying force effectively resulted in less broken sutures and loose knots. However, the system suffers from errors due to wrist actuation and friction.

Hagen et al. [35] concluded that the idea of the haptic feedback increases with experience of the robotic surgery. During the study, mostly the inexperienced surgeons showed the concerns related to the haptic feedback whereas the experienced surgeons picked the visual clues from the visual feedback from the system that acted as analogous to real haptic feedback. Wagner et al. [36] whereas motivated the use of force feedback with the aim to reduce the mental workload and control accuracy required to carry out a task during the operation.

An experimental study was carried out by Wagner et al. [32] in which the participant surgeons were asked to dissect and expose the arterial structure inside the tissue by using tele surgical robot consisting of two PHANToM® haptic controllers. They concluded that the presence of the force feedback decreases the number of errors in the tasks. However, it did not affect much on the speed of the process. A similar conclusion was made in a similar kind of experiment conducted by Deml et al. [37]. It is also hypothesized that force information gets transformed from physical constraint into additional details when force feedback levels get reduced. A conscious effort is required to utilize the additional information.

Wagner et al. in [38] explained that the additional information generated with a decreasing level of force feedback is utilized by the trained surgeons only without an increase in trail time. This

also concluded that force feedback reduced the error in the system without much attention and did not increase the mental load.

The literature mentioned above discusses the advantages of the force feedback system that leads to the reduction of applied force level, but none of them proved a reduction in task execution time. Some of the theories hypothesized that haptic feedback is only limited to specific applications, questions still are raised, whether the high-quality feedback is needed or not and whether feedback of all force and torque components is necessary.

Kitagawa et al. [39] indicated that the force feedback effect is only limited to 2 DoF because the force along the tool shaft is approximated. 3 DoF force feedback improves the user performance close to the performance of open surgery. A modified EndoWrist® with a 6 DoF equipped with ATI-Nano force sensor when an attempt was made to determine all the force components during the operation [41]. The study assumed that the element of force with the most substantial magnitude is the most significant one, but the validity of the assumption is not proven yet.

2.8. Advantages of Impact Modelling

In the present minimum invasive robotic systems (MIRS), the surgeon estimates and provides the input to the surgical arm in the form of position/velocity to interact with the environment. The latency in the process of the teleoperation makes the realization harder to estimate the contact. The

input is considered to be known to the surgical arms with a capability of operating in an autonomous mode. A novel approach is developed by using MPC as a position controller to obtain minimum impact on the environment in a teleoperated system to prevent accidental damage to the environment.

2.9. Imaging in the Surgical Robots

In MIRS because of the small incisions and camera views, the surgeon no longer can see the operation directly. Visualization is one of the critical processes for these systems as the surgeon operates from a remote location and relies entirely on limited field-of-view video of the operating room. Especially for the case of telerobotic surgery, the video suffers from latency depending upon the distance between master and slave end. The perspective of the current time *t* comes with a time lag to the surgeon. With the advancement in the camera technology, now surgeons can see on a 3D image where tracking their surgical tools concerning lesion responsible for patient's problems.

The 3D imaging is compressed and coded first at the remote site and then transported to the master end via a communication medium and decoded again. This process of coding, decoding of the video of the operating site takes time in the range of 550 ms – 850 ms for a current time step *t* [49] . On the other hand, this means that the surgeon sees the perspective of the current time step at the slave end after almost 550 ms (minimum). This latency is the sum of the time taken by the computing systems to code, decode the video and the data delay in transmission.

One of the aims of this research is to develop a simple kinematic predictive imaging such that the surgeon can get a delayed free simulated image of the robotic arm operating on the environment. We have assumed that the data delay is constant throughout the process that must be relaxed later.

2.10. Structure of Bi-Lateral Teleoperated System

The block diagram is shown in Figure 11. describes bilateral teleoperation system [76]. A typical telesurgical system can be divided into three parts: master system (local environment), remote environment (slave system), and the communication channel in between.

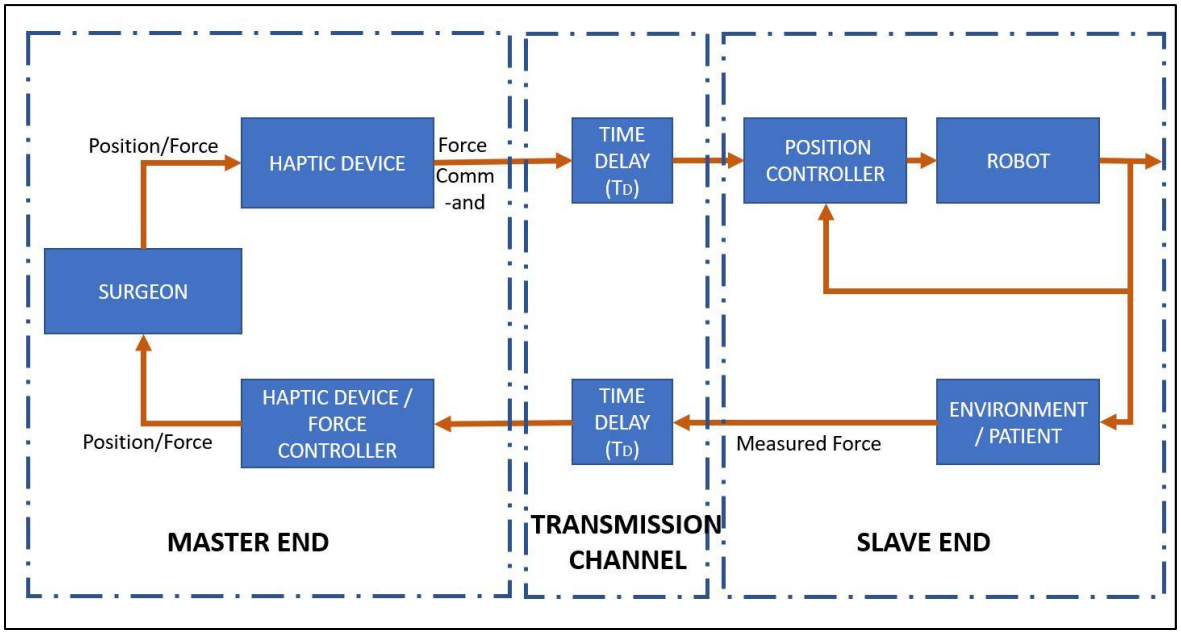

FIGURE 10: BLOCK DIAGRAM OF THE BI-LATERAL COMMUNICATION IN MASTER/SLAVE TECHNOLOGY

MASTER SYSTEM

The master end of the surgical system allows the surgeon to command the surgical robot and perform the surgery. The prime responsibility of this end of the system is to provide accurate and realistic visualization of the operating area located at a remote site. This end of the system provides an intuitive and ergonomic working environment for the surgeon to carry out the process.

The master system comprises a surgeon and haptic device. The surgeon commands position/force signals to the slave end through the communication channel. Most of today's commercial medical master systems can't provide force feedback or tactile feedback to the surgeon.

A surgeon sitting at the master console end also gets visual feedback from the environment generated by laparoscopic cameras displayed on the video screen. The current surgical arms have a well-developed 3D stereoscopic vision system. DLR arm can give the surgeon an impression of the remote forces even though it does not have any force feedback to the input devices [77].

COMMUNICATION CHANNEL

Master console is connected to the slave robot through a communication link in the process of teleoperation. Mostly, for the application of teleoperation broadband technology is used to connect the surgeons to the virtual hospital. Each surgeon uses his desktop without interacting with his

assistants. Depending on the distance between the local site and the remote site system suffers from communication delays T_d (*sec*) in the forward as well as feedback loop as described in Figure 11. The delay can be variable or constant and cannot be avoided in the communication medium.

Internet or wireless 802.11 networks is considered very interesting for the long-range communication. However, Internet protocols unreliability hinders [78] their use in the bilateral communication. Losses and delays in the network introduce additional complex dynamics that can lead the system to instability. They suffer from random delays that affect [79] the control performance of the system and must be considered while designing the control algorithm [80]. The variation in the time delay can be reduced can be reduced by using buffers and waiting strategies [81].

Network communication system and wireless links are never delayed free and offer limited bandwidth in the practical scenarios. Hence the network systems have a negative impact on the performance of the system owing to their random behavior. The total time delay in a system comprises of the following components: communication delay, data loss and sampling delays as shown in Figure 12.

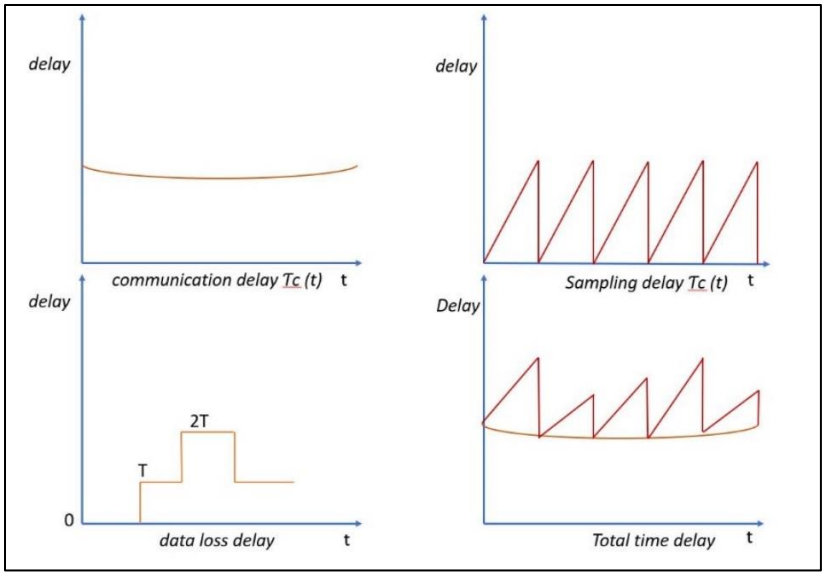

FIGURE 11: NETWORK DELAYS

Where T_c denotes the time delay due to communication and T_s is the sampling delay in a system. For the case when the sampling period is constant, the data loss delay is N_T, where N is a positive integer. The total time delay in a system as one type of variable delay can be termed as T (t) as described in equation 2.1 :

$$T(t) = Tc\ (t) + Ts\ (t) + N_T \qquad (2.1)$$

Network delays are very fast time-varying, constant delays are rather the approximation of the practical situation. Various other sources of delays can be detailed as follows:

1. Depending on the types of the internet, communication delay can be bounded or unbounded. For example, local area network introduces bounded communication whereas internet leads to unbounded communication delays leading to packets drop out.

2. The synchronization in between the masters and slaves clock is also another source of time delay, but this effect is neglected in most of the situations by assuming a proper synchronization between both the ends.

3. Bilateral communication is two-way communication between the master and slave ends. The forward channel and the backward channels constitute delays which are asymmetric. To simplify the process, the delays are considered symmetric, but in practical conditions, they are not since routers and path are not always the same during the communication.

4. The information is also lost when the data is transferred [82] from one end to another that is termed as packet dropouts rate. This term indicates the number of packets dropped and that do not reach the destination. The transmission errors in the network system and overflow of the buffer due to network congestion are the main causes that lead to packets drop out.

5. TCP vs., UDP (Time Control Protocol vs., User Data Protocol). In a control situation, every data packet contains some set of vital information containing the vital values of measured position/velocity/force. If a packet gets lost during the communication, we can choose to resend it corresponding to TCP. However, this may lead to network congestion. The more

convenient way is to send next sampled value without resending the lost one that is supported by UDP.

SLAVE END

This section focuses on the remote end of the surgical robot that is known as Slave end. The function of the slave robot is to follow the master's command efficiently and provide seamless visualization of the operating room. The current instruments for the MIRS distinguish from conventional MIS as handles got substituted with electrical drives. The slave end has following other capabilities too:

1. Additional DoF inside the body.
2. Combination of multi-functional instruments, e.g., scalpel and forceps.
3. Laparoscopic vision.
4. Force and torque measurement.

In the open surgery, the surgeon's hand's dexterity inside the human body can be matched with that of MIRS by using additional degrees of freedom at the tooltip. The operation becomes a lot safer and faster with the introduction of additional DOF.

Chapter -3
Model Predictive Control

MPC (Model predictive control) is a well-known control strategy used nowadays that has gone through a lot of evolution, due to its ability to handle the system's shortenings robustly. The work was started by Kalman in '60s [52] when working on a controller with the aim to find an optimal input for a linear model by quadratic penalization with an infinite horizon of states and inputs. This model is known as linear quadratic regulation (LQR) [53]. LQR is not a famous control strategy amount the industrial control specialists owing to its limitations. One of the limitation is the absence of constraints in the formulation of the problem. LQR doesn't perform well when the system is non-linear or have large time delays in it. Freedman and Bhatia in 1985 [54] started using Dynamic Matrix Control (DMC) in the chemical and petrochemical fields. In the area of chemical industry, the products are measured in kilo or megatons, even a small improvement in the area of controls will lead to huge savings. This approach was successful enough in the processes where the process dynamics are slow. The optimal input is computed based on optimization performed in less time than sampling time of the system. Initially, the stability was not determined theoretically. The first version of MPC was not able to stabilize the process automatically, but long prediction horizon and stable systems were used to use and improve the approach. Generally, the optimization problem is always predefined in the system while aiming at finding necessary state values. MPC use observers to estimate the states of the system since all the states in system are not measurable. To control the process that has fast dynamics so-called approach Explicit Model Predictive Control was introduced [55]. Apart from the other advantages of the traditional MPC, this type of MPC can be implemented on the systems with weaker hardware. The optimization

problem is solved on offline phase using parametric programming, only the function evaluation is carried out on online mode.

The intuitive approach of MPC imitates the humans complex control system. Humans don't rely only on the power transfer computation and reactions from the sensory system, but the original approach is based on knowledge of results of the actions on the future consequences. This process of learning in the humans developed with time and stored in the memory such that it is utilized when required. Many models have been proposed to describe the learning pattern of human behavior but are not fully developed yet. The way how the learning is used to predict the future is even more complicated.

3.1. MPC for time-delayed systems

For delay-free systems, the MPC has huge literature available showing its effectiveness towards stability and capacity to handle uncertain dynamics of the system with and without constraints on them. It shows a good tracking performance overall [56] [57] [58] [59] [60] [61] [62] [63]. MPC can be used to reduce input-delayed system to a delay-free system as in [68][67], but there are only few MPC algorithms to control delayed time system because infinitely dimensional systems are hard to control and handle.

In 1996, Kothare and his co-authors [64] concluded that the proposed MPC control scheme for the delayed free system could be extended to the linear time-varying state-delayed system by having

an equivalent augmented delay-free system. Later, Richard pointed out [65] that the approach presented earlier is not valid for the time-delayed system as it leads to a high degree of complexity. Another simple receding horizon control scheme was suggested that reduces the optimal problem of state delay systems into the optimal problem of delay-free systems [66]. However, the authors admit that the closed loop stability is not guaranteed by the proposed control scheme.

In 2003, Kwon [67] [68] proposed a general MPC scheme for time-delayed systems. Here the "general" depicts cost function that must be minimized over the horizon, and closed-loop stability is guaranteed. This proposed cost function includes state and the input weighting terms unlike other functions [69]. The optimization algorithm proposed is a generalized form of Riccati equation. A condition is applied to the terminal weighting matrix for the MPC in the form of linear matrix inequality(LMI) which guarantees that the optimal cost is monotonic for the delayed system. This proposed scheme can only be applied to the linear systems with single time delay. Jeon and Park [70] extended the above scheme to random time delays in the discrete-time domain.

Hu and Chen [71] proposed MPC algorithm for the constrained systems with uncertain time delays. The scheme consists of two algorithms. One of the algorithms works on off-line mode and other works on online mode. The proof of the stability of the algorithm is not concrete.

The literature to the control of nonlinear systems with time delay using MPC is minimal. Mostly, the delays are considered in linear terms than nonlinear terms [72] [73] [74]. Kwon et al. [75] also proposed a scheme for nonlinear state delayed systems. A terminal weighting function was

introduced to achieve the closed-loop stability. The author also mentioned that it is difficult to find the control law based on their control algorithm.

3.2. Comparison of MPC to other Approaches

Classic control in comparison to the MPC has several weaknesses. Proportional-Integral-Derivative (PID) control one of the most widely used controllers owing to its easy control structures, and gains can be changed by operators to improve the performance of the system. PID does not provide optimal control inputs. However, the input to the system can be saturated mechanically, but it causes destabilization of the systems.

More advanced control, Linear Quadratic Regulator (LQR) provide us with optimal control inputs [57]. LQR solves the optimal control problem (such as Riccati equation) of minimization the states and inputs over the infinite prediction horizon. The optimization problem is subjected to the linear system over linear constraints. MPC has the ability unlike PID can handle MIMO (multiple inputs multiple outputs) systems and can also manage system with constraints of types equalities and inequalities. MPC, unlike LQR, uses finite prediction horizon the benefits coming from the constraints satisfaction making the control interesting [58] [59].

3.3. Model Predictive Control components

Model predictive control (MPC), which is also known as receding horizon control (RHC) has gained the attention of the researchers because of its unique advantages. The advantages include [61]:

- Computational feasibility.
- Applicability to a broad class of systems.
- Wide acceptance in industrial applications.
- Guaranteed stability of a closed-loop system through a systematic approach.
- Robustness in tracking the performance of the system concerning system modeling as well as external disturbances.
- To handle the controls with hand and soft constraints on systems states.

The MPC works on the strategy that aims to perform the optimization problem over a finite prediction horizon to predict the future control sequences. MPC exploits the predictions from the output of the process model to find the future control events by coping with amplitude and constraints on the inputs, outputs, and states. PID control can react to the past behaviors whereas MPC can anticipate the future behavior of the system. The control strategy of driving a car is very close to the approach of MPC [61] as shown in Figure 13.

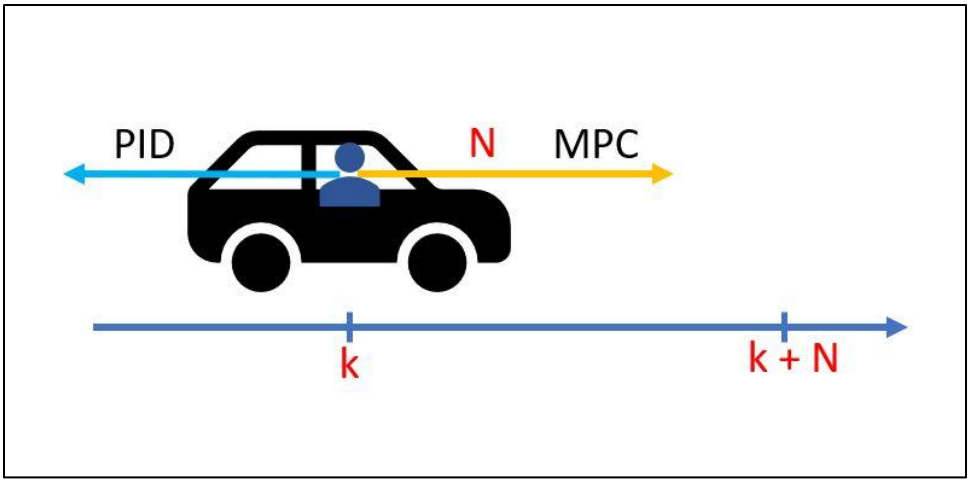

FIGURE 12: THE COMPARISON BETWEEN MPC AND PID CONTROL

At the time instant k, the driver knows the desired reference for a fixed interval called finite control horizon [from k, k + N]. The driver knows the control measures (braking system, steering and gas pedal) to consider such that the car follows the desired path. The first control law is considered as the current control law only, and the process is repeated over the next time horizon, say [k+1, k+1+N]. The method of shifting of horizon after every time step is called as the receding horizon principle. Figure 14 shows the basic MPC's control strategy.

The MPC predicts the future plant outputs by using a systems model. The optimal future control actions are proposed based on the past and present values. These actions are evaluated at each time step by the optimizer by keeping into account the cost function of the system, along with the constraints on the system. The model must be well defined such that the entire future values are well based upon the model of the system.

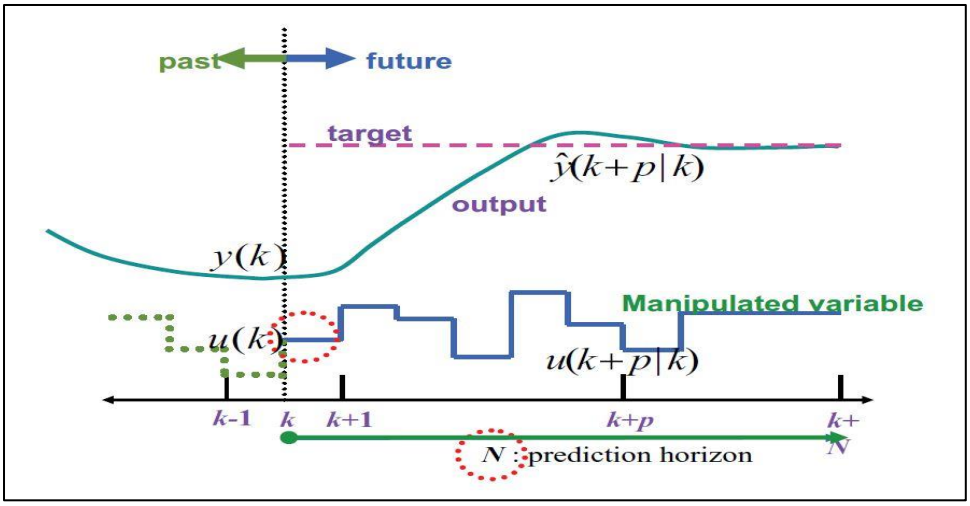

FIGURE 13: MPC CONTROL APPROACH [61]

There has been extensive research on the use of MPC on the delayed free systems [62] as compared to the time-delayed systems.

3.4. Model Predictive Control Formulation

Model predictive control consists of the following components [90]:

- The objective(cost) function,
- Constraints in the form of equalities and inequalities,
- Initial conditions.

The primary objective of the cost function is to minimize the error between the prescribed references and plant's states accounting for minimization of consumed energy [56]. The mathematical model or the transfer function of the system enters the optimization problem as equalities constraints. The Limits on the state variables i.e., manipulated variables and manipulated

are considered as the inequalities constraints. The problem forms a convex set if all the constraints are linear. MPC can be solved as a convex optimization problem if the objective function is also convex. Similarly, if the MPC problem is considered as a quadratic problem if the objective function is a quadratic problem.

In the open loop implementation of the process, the whole control action is applied to the system, and the next measurement is done after the last part of a computed control sequence is applied. In the end, the optimization problem is solved again. Open loop implementation looks a good way of implementing the MPC but if something unexpected happens in between the two measurement steps, the controller does not know how to handle the unexpected event because of unavailability of information at the time of prediction whereas in closed loop implantation the entire controlled sequence is not implemented to the process but only the first element. The optimization problem is repeated after the measurement is performed.

3.5. Optimization Problem

MPC uses the model of the system to predict the response of the controller based on the future events [63]. Then the optimization process is carried out to find the best control input to get the desired output response of the system as shown in Figure 15. We will consider a linear time-invariant system in the discrete time domain as shown in (3.1):

$$x^{+} = Ax + Bu \tag{3.1}$$

where,

$x \in R^{n}$ is vector of states.

U $\in R^m$ is vector of inputs.

x^+ is the successor state at the time interval.

The system represented by equation one is assumed to operate with the following constraints: -

$$x \in \boldsymbol{X}, u \in \boldsymbol{U} \tag{3.2}$$

where,

$$\boldsymbol{X} \subseteq \mathrm{R}^n \text{ and } \boldsymbol{U} \subseteq \mathrm{R}^m$$

Also, we assume

$$\boldsymbol{X} = \{x \mid Hx <= K\} \tag{3.3}$$

$$\boldsymbol{U} = \{u \mid Lu <= M\} \tag{3.4}$$

where (3.3) and (3.4) are half-space representations of constraints on the state and input variables. The standard cost function regarding Quadratic Program(QP) is the sum of terms as shown in (3.5), each term aims at an aspect of the control performance [69].

$$J(z_k) = J_y(z_k) + J_u(z_k) + J_{du}(z_k) + J_e(z_k) \tag{3.5}$$

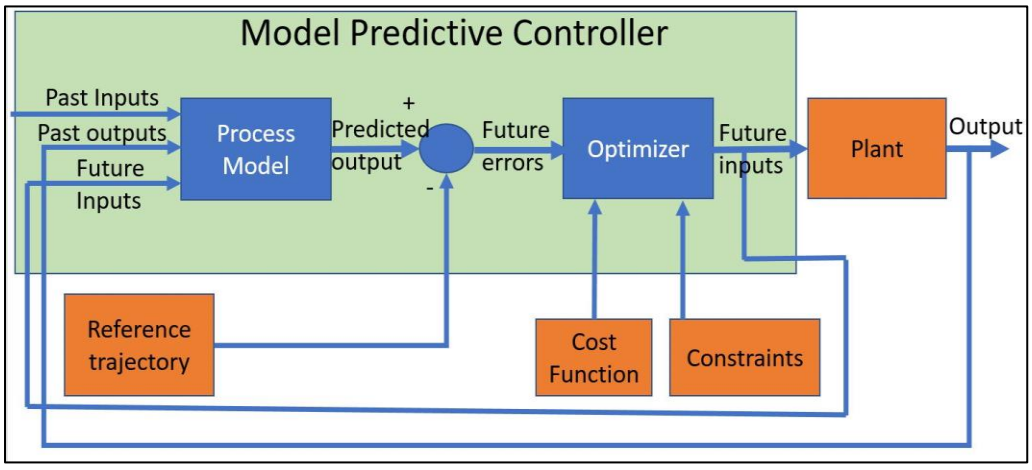

FIGURE 14: STRUCTURE OF MPC

Here as_k is the decision from the QP that is evaluated at every time step. When the MPC controller is initialized the system contains default weights on each term. Each term as shown in the equation (5) includes weights that can be adjusted to achieve the desired objectives.

3.5.1. Output Reference Tracking

The controller must keep the plant outputs close to that of specified reference values. MPC Controller the scalar performance measure showed in (3.6) for output reference tracking [69].

$$J_y(z_k) = \sum_{j=1}^{n_y} \sum_{i=1}^{p} \left\{ \frac{w_{i,j}^{y}}{s_j^{y}} \left[r_j(k+i|k) - y_j(k+i|k) \right] \right\}^2 \qquad (3.6)$$

where:

k- Current control interval.

p- Prediction horizon (number of intervals)

b_y – Number of plant output variables.

Z_k - QP decision, given by:

$$z^T_k = [\, u(k|k)^T \;\; u(k+1|k)^T \;\; \ldots\ldots \; u(k+p-1|k)^T \; e^k \,].$$

$y_j\,(k+i|k\,)$ – the Predicted value of j^{th} plant output at i^{th} step.

$r_J(k+i|k\,)$ – Reference value for j^{th} plant output at i^{th} step.

$s^y{}_j$ – output scale factor.

$w^y{}_{i,j}$ – Tuning weights for the plant output.

Here n_y, p, $s^y{}_j$ and $w^y{}_{i,j}$ is the controller's specifications that remain constant throughout the process. The reference, $r_j(k+i|k\,)$ is provided to the controller such that it can predict the plant output $y_j(k+i|k\,)$ by using state observer at each time step k. The state observer manipulates the

manipulated variable (MV) (z_k), measured disturbances (MD) and state estimates to get the optimal performance for a system.

3.5.2. Manipulated Variable Tracking

Manipulated variables are the controlled outputs generated by the controller at each interval, *k*. In the cases when there are more manipulated variables than plant outputs, MPC must keep selected manipulated variables (MVs) near the target values. MPC controller uses the following scalar measure as shown in (3.7) for manipulated variable tracking [69].

$$J_{du}(z_k)=\sum_{j=1}^{n_u}\sum_{i=1}^{p-1}\left\{\frac{w_{i,j}^{du}}{s_j^u}\left[u_j\,(k+i|k)\;-\;u_j(k+\;i-1|k)\right]\right\}^2 \tag{3.7}$$

where:

k- Current control interval.

p- Prediction horizon (number of intervals)

n_y – Number of plant output variables.

z_k- QP decision, given by:

$$z^T{}_k = [\,u(k|k)^T\;\; u(k+1|k)^T\;\ldots..\; u(k+p-1|k)^T\; e^k\,].$$

$u_{j,target}\,(k+i|k)$ – Target value for jth MV at ith prediction step

$s^y{}_j$ – output scale factor.

$w^y{}_{i,j}$ – Tuning weights for the plant output.

Here n_y, p, $s^y{}_j$ and $w^y{}_{i,j}$ are the controller's specifications that remain constant throughout the process. The controller uses the $u_{j,target}(k\;+\;i|k)$ values for the entire horizon that is used to get the systems output close to the desired values.

3.5.3. Manipulated Variable Move Suppression

Most of the applications prefer small MV adjustments as shown in equation (3.8) [69].

$$J_u(z_k) = \sum_{j=1}^{n_u} \sum_{i=0}^{p-1} \left\{ \frac{w_{i,j}^u}{s_j^u} \left[u_j\,(k+i|k) - u_{j,target}(k+i|k) \right] \right\}^2 \qquad (3.8)$$

where:

k- Current control interval.

p- Prediction horizon (number of intervals)

n_y – Number of plant output variables.

z_k- QP decision, given by:

$$z^T_k = [\, u(k|k)^T \;\; u(k+1|k)^T \;\; \ldots\ldots \; u(k+p-1|k)^T \; e^k \,].$$

$w^u_{i,j}$ – tuning weight for the input.

s^u_j – input scale factor.

Here n_y, p, s^y_j and $w^y_{i,j}$ is the controller's specifications that remain constant throughout the process.

3.5.4. Constraint Violation

Constraint violations might be unavoidable in actual practice. An MPC controller employs a slack variable which is positive dimensionless quantity quantifying worst case scenarios. Equation (3.9) is the corresponding performance measure.

$$J_e(z_k) = \rho_e \; e_k^2 \qquad (3.9)$$

where:

z_k - QP decision, given by:

$$z^T_k = [\, u(k|k)^T \;\; u(k+1|k)^T \;\; \ldots\ldots \; u(k+p-1|k)^T \; e^k \,].$$

e^k - slack variable at control variable k.

ρ_e – Constraint violation penalty weight.

Chapter 4
Control Formulation

4.1. Contact Force Control

The robotic manipulator at the slave end contacts the environment while executing a task. It is essential to control the contact forces accurately not only to successfully achieve the work but also the mutual safety of the patient in the environment, robot, and humans present around the environment. The motion of the robot during in contact with the environment is not accurate and precise due to the presence of uncertainties in the model of the robot and environment. It is necessary to have compliant control strategies to control the contact forces that will ensure safe interaction with the environment especially in the case of surgical robots.

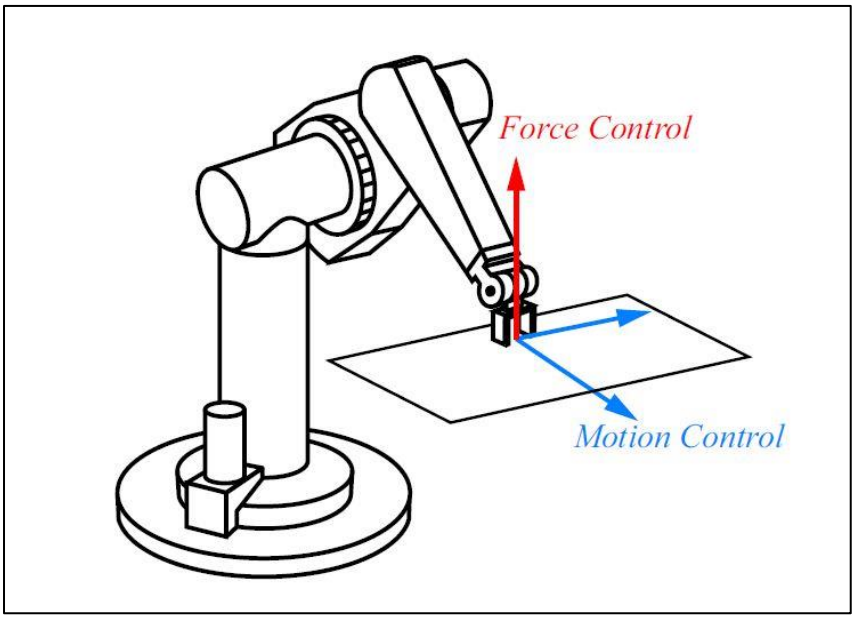

FIGURE 15: FORCE CONTROL DIRECTION [84]

Compliant control strategies can be categorized as direct force control and indirect force control. Indirect control strategies try to achieve the desirable compliance state at the end of the effector's contact point in the contact direction. The direction perpendicular to the point of contact is chosen to be complaint direction as shown in Figure 16. The proportional gains for the compliant direction are selected to get the desired stiffness and to achieve the desired position control in other directions, gains are determined accordingly. Indirect control strategies can be classified into stiffness control [83] and impedance control [84] depending upon the behaviors of the system.

Direct force control relies on the control law that uses the error between desired and measured contact forces than the position errors. Impedance control relies on the stiffness measurement of the environment to generate the desired force at the end of effector, i.e., explicit control of the contact forces. In practical scenarios mostly while operating inside the human body, the stiffness varies from few kPa to several hundred kPa depending on the tissues operating on [85] as illustrated in Figure 17.

In direct force control strategies, an external feedback loop is created outside the position loop [86]. The external feedback to the force controller helps to correct the input to the motion controller. Proper knowledge of the contact environment is required to design a proper controller. Hybrid position/Force control and operational space approach are the two approaches that are used in the direct force control strategies. Operational space approach provides more flexibility for the design of the controller than any other approaches.

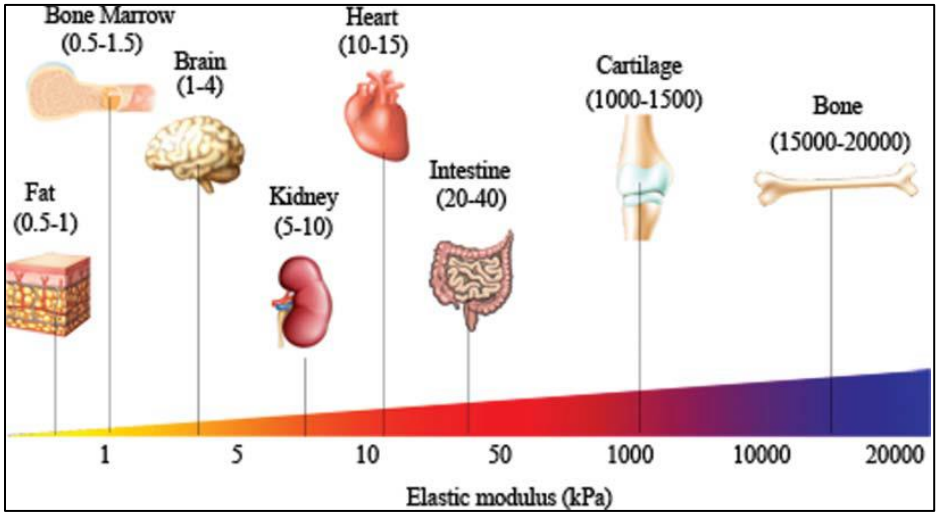

FIGURE 16: DISTINCT MODULUS OF HUMAN TISSUES SUGGESTING TISSUE-SPECIFIC STIFFNESS [85]

External Hybrid force/position control approach is considered in this thesis to prove the concept. Typically, proportional-integral (PI) control is used in force control applications to ensure zero steady-state errors. However as discussed in chapter 3, PID cannot control the time delay in a system when time delay exceeds time constant. As a result, the MPC controller will be used as a force control to develop this novel approach as it can predict the future and can handle the time delay effect. The development of the force controller using the hybrid force/position control is the focus of the chapter. Two different situations have been considered to develop the force control under the deterministic time delays. Simulation study for the force controller is conducted for one-point contact at the end of the effector. The position control controls the other translational direction.

4.2. Implicit force control

4.2.1. Passive compliance control

A simple mechanical solution to reduce the external forces on the manipulator from the environment is given by Whitney and Nevins [87] based on the deformable mechanical interface. The physical configuration of the mechanical device attached to the end-effector changes when in contact with the environment. The elastic behavior gets added to the structures that are compensated by the position controller as shown in Figure 18.

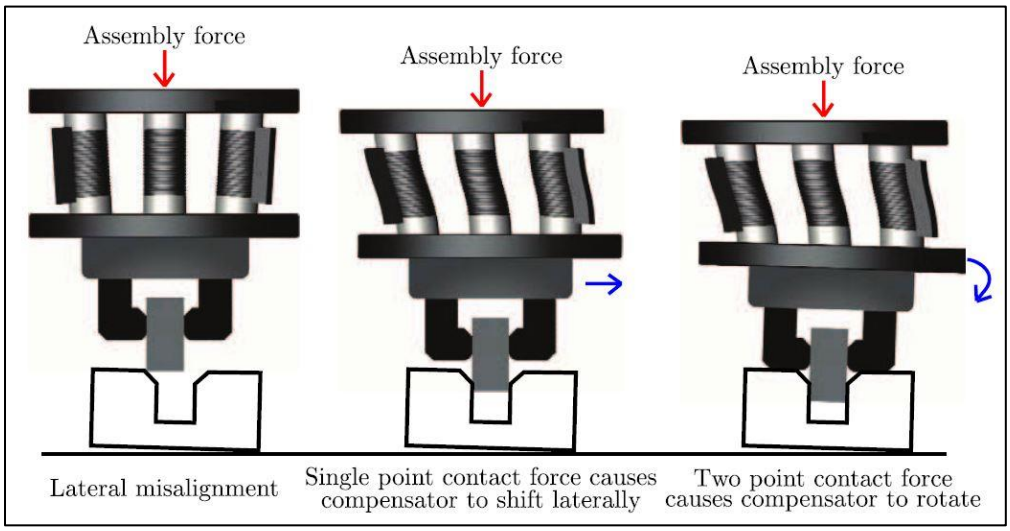

FIGURE 17 : COMPLIANCE CONTROL

(SOURCE: WWW.ATI-IA.COM).

Compliance control is a simple control strategy involving fast and accurate insertions of the parts. The compliance device is specially designed for a specific task and workpiece making it one of the limitations of this kind of control.

4.2.2. Active stiffness control

This method controls the position and forces simultaneously along with the stiffness of the end-effector. The system acts a simple spring model with variable stiffness, such that system reduces the contact forces between the system and environment during interaction phase [88]. A compliance frame can be specified by the user that contains three translational and three rotational components. The relation between displacement dX and resultant force f is given by the equation (4.1).

$$f = K_s \, dX \tag{4.1}$$

Where K_s is the desired stiffness. The relation between the force f in the Cartesian space and torque τ in the joint space is given by equation (4.2). It is assumed that the friction and dynamic forces are compensated or are small enough such that they can be neglected.

$$\tau = J^T f. \tag{4.2}$$

Displacement in the Cartesian space given in joint space

$$dX = J \, dq \tag{4.3}$$

combining equations (4.1), (4.2), and (4.3) gives us

$$T = J^T K_s J\, dq = K_p\, dq \tag{4.4}$$

Where K_p is the joint stiffness matrix.

4.2.3. Impedance control

Impedance control considers the robot like a mechanical impedance *Z(s)* and assign a dynamic behavior when the end-effector is interacting with the environment. Dynamic impedance representing the mass-spring-damping system specifies the dynamic performance.

The relation between the end-effector and contact forces is given by:

$$F(s) = Z(s)\, \Delta X(s) \tag{4.5}$$

Where $\Delta X(s)$ is the displacement in the operational space and *F(s)* is the force due to interaction with the environment. Depending upon the different phases of the task, the impedance of the system *Z(s)* is variable. The general form of the impedance control is given by mass-spring-damping system with the following transfer function:

$$Z(s) = Ms^2 + Bs + K \tag{4.6}$$

Where *M*, *B*, and *K* are the desired inertia, damping and stiffness matrices. The values of these matrixes are selected based on the desired performance measures. High costs are chosen for the matrix *M* in the direction of the expected contact to limit the dynamics of the robot. The values of stiffness *K* affects the position controllers precision. It should be small enough along the movement of the manipulator and should be kept high for accurate positioning of end-effector. The value of damping constant *B* is selected as per the damping required in the direction.

Two control structures are available for the impedance control depending upon the availability of the force sensor [85].

The first one computes force 'applied' using relation (4.5) by measuring the position as in Figure 19.

The second control structure uses the values from the force sensor to measure the interaction forces that is translated to position feedback as in Figure 20.

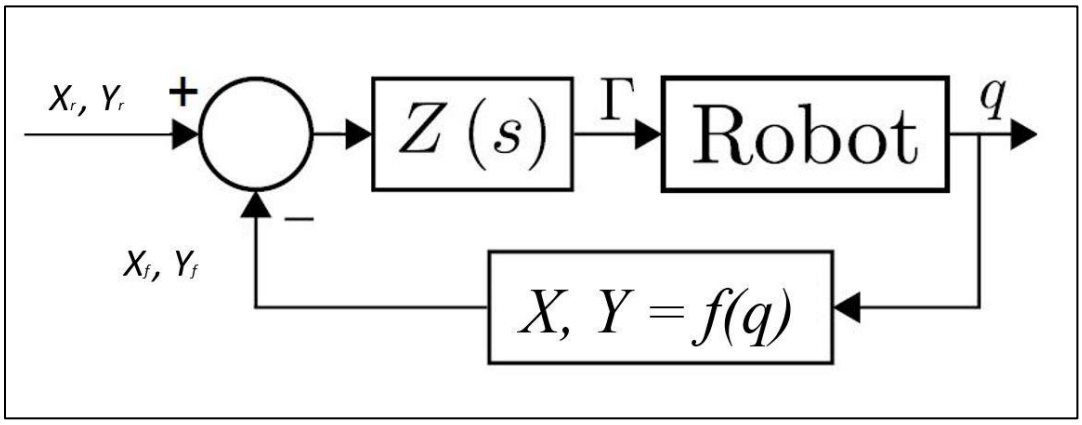

FIGURE 18: IMPEDANCE CONTROL WITHOUT FORCE SENSOR

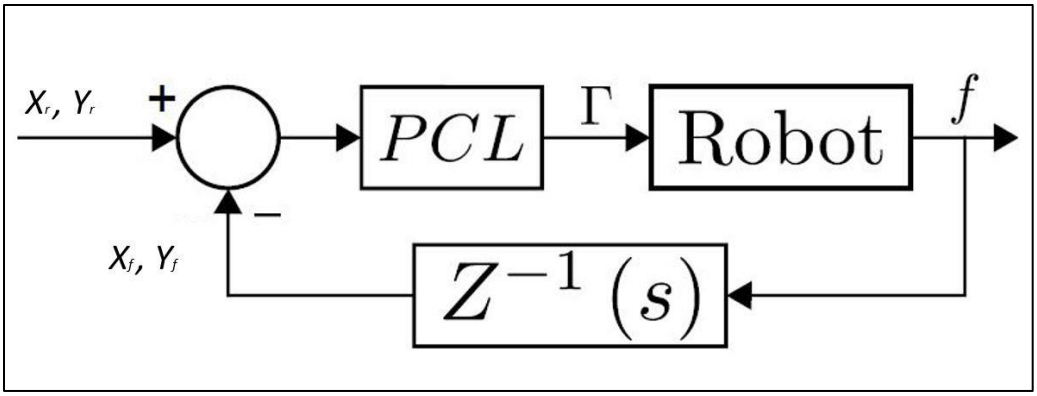

FIGURE 19: IMPEDANCE CONTROL WITH FORCE SENSOR

Implicit controllers help to control the change in dynamics of the robot when in contact with the environment than controlling the direct force that's applied to the situation. In other words that means the reference is not forced to the control law. Explicit controller deals with the classical force controllers with direct feedback from the environment.

4.3. Explicit force control

4.3.1. Hybrid position/force control architecture

Raibert and Craig [90] proposed a hybrid law in which the workspace is divided into two subspaces: position is controlled in one direction and force is controlled in other direction. In this control law force and position cannot be controlled for the same direction. The directions that are force constrained are position controlled, and the directions that are position constrained are force controlled.

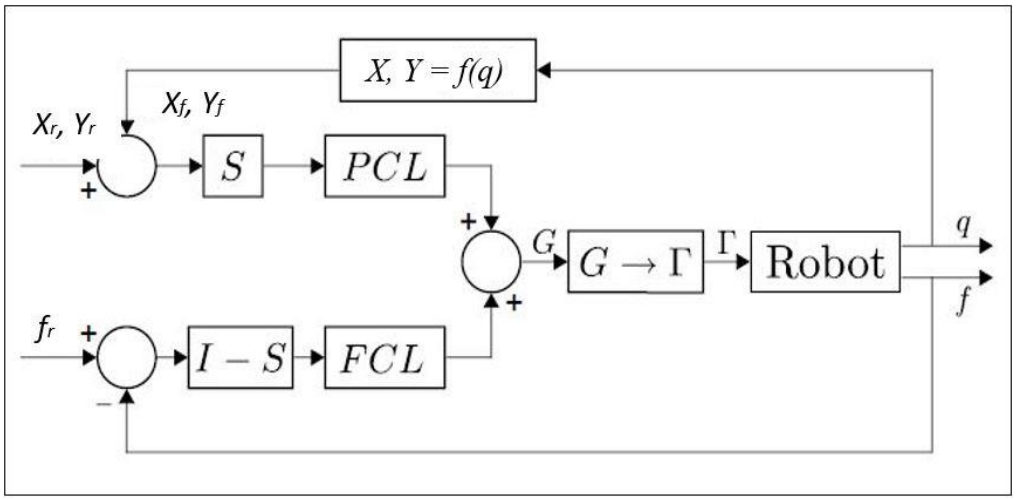

FIGURE 20: HYBRID POSITION/FORCE CONTROL LAW

The control law consists of two loops; the internal loop is position controlled loop whereas the outer loop is the force-controlled loop. To avoid the actuator conflicts between the two control loops a compliance selection matrix S is used. G is the controlled input sent to the robotic manipulator from the controller. The controlled input G can be either the joint torques T directly to the robot's actuator or can be equivalent to velocities or displacement in cartesian or joint coordinates.

Figure 21 shows the hybrid position/force control architectures where PCL is Position Control Law, and FCL is Force Control Law. This control law allows to control the position and force with explicit feedback but still they require the well-known environment to avoid instability.

4.3.2. External hybrid force control

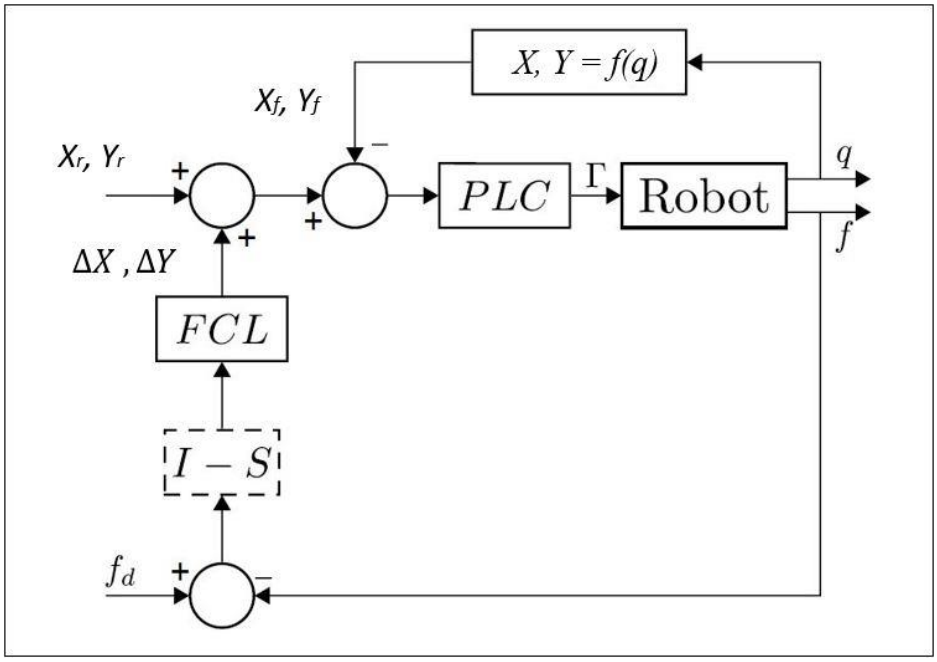

FIGURE 21: EXPLICIT HYBRID POSITION/FORCE CONTROL LAW

The external hybrid position/force control architecture allows control of the force and position in the same direction unlike parallel hybrid position/force control as shown in Figure 22.

It contains two embedded loops, one external loop for controlling the force and another internal loop for a position loop. The controller transforms the desired force into a position that gets added to the desired position. The new position reference is sent to the position controller. The displacement calculated from the force controller allows the system to apply force on the environment. This kind of architecture does not require any selection matrix. This control law always has an integral term to remove the steady-state error for the desired position. When the environment is not known, it is quite hard to keep force directions controlled in position preventing

contact forces in case of undesired contact: displacements are controlled by force consign. This approach has a drawback such that instability occurs when the force consign is close to zero.

The state space realization of the system with a delay in the input and output at the slave end is given by the equations (4.7) and (4.8).

$$X = A\,x(k) + BU\,(k - t) \tag{4.7}$$

$$Y = C\,x(k) \tag{4.8}$$

Where A, B, C are the state space matrixes for the robotic manipulator.

4.4. Kinematic Predictive Imaging

With the advancement in the video technology, there have been considerable improvements in the vision available to the surgeon at the master end. This vision requires high bandwidth and low latency to get transmitted from slave to the master end, unlike the available public network domain.

Hence the video suffers from time delays and losses during the transmission of the data. Secondly, on the top of this problem, the latency incurred by the data transmissions is in the range of 70 - 300 ms whereas visual delay generally ranges from 550 ms – 850 ms [49]. The image is converted to the low-resolution imaging by coding at the remote end and is transmitted than in the form of

data to the master console where the low-resolution image is decoded to the high resolution and displayed at the master console. If we assume that if data delay is 80 ms, visual delay due to computational load is almost 220 ms each side of the robot.

In other words that means at a time instant *t* during the surgery, the surgeon gets the perspective of the operating room after almost 400 ms (let consider visual delay (550 ms) = latency due to computational load + data delay). As a result, the surgeon gets an optical output on the master console after 400 ms for the current timestamp.

This is one of the main reason that makes the MIRS time consuming as compared to the open surgery. Moreover, The contact of the slave robot with the environment can get unstable due to lack of perception for the current time *t*. This can damage the environment on which the operation is carried on.

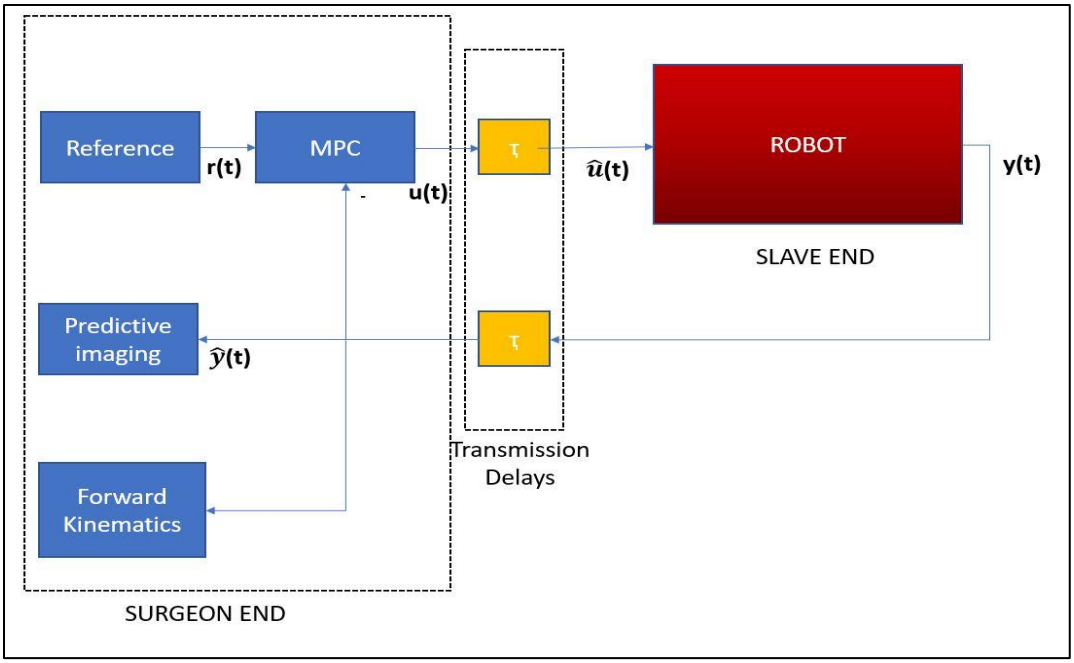

FIGURE 22: SYSTEMS ARCHITECTURE FOR PREDICTIVE IMAGING

This part of the chapter looks into developing a novel approach to have some form of predictive imaging without any delay at the master console. It is assumed that the robot is operated in a known environment. Figure 23 shows the system architecture of the predicted imaging using an MPC at master end.

MPC is used as a position controller at the master end such that the output in the form of joint coordinates is required at the master console itself. This signifies that the output suffers from two-time delays in this application of imaging. The model predictive control should be able to compensate the time delay and its effects in the system to produce a predicted output at the master console.

We have assumed a simple dynamic model of the robot without the actuators model to carry out the initial testing of this concept. The formulation of the robot present in chapter 5.

Steady space realization of a time delayed system with input and output delay as represented in the Figure 23 is given by equation (4.9) and (4.10) as the input and output of the system are at the master end .

$$X = A\,x(k) + B\,U\,(k - t) \tag{4.9}$$

$$Y = C\,x(k - t) \tag{4.10}$$

Where A , B , C are the state space matrixes for the robotic manipulator.

4.5. Model Predictive Control Formulation

The controlled output of the model predictive control can be defined as in equation (4.11):

$$\tilde{u}_k = \Delta\ \tilde{u}_k + u_{k-1} \tag{4.11}$$

General steady state equation is represented by equation (4.12):

$$X = \tilde{A}\,x(k) + \tilde{B}\,U \tag{4.12}$$

which, more specifically, takes the following form:

$$\begin{bmatrix} x_0 \\ x_1 \\ x_2 \\ \vdots \\ x_{N-1} \end{bmatrix} = \begin{bmatrix} I \\ A \\ A^2 \\ \vdots \\ A^{N-1} \end{bmatrix} x(t) + \begin{bmatrix} 0 & 0 & \cdots & \cdots & 0 \\ B & 0 & \cdots & \cdots & 0 \\ AB & B & 0 & \cdots & 0 \\ \vdots & \ddots & \ddots & \ddots & \vdots \\ A^{N-2}B & A^{N-3}B & \cdots & B & 0 \end{bmatrix} \begin{bmatrix} u_0 \\ u_1 \\ u_2 \\ \vdots \\ u_{N-1} \end{bmatrix} \tag{4.13}$$

where,

$$X = \begin{bmatrix} x_0 \\ x_1 \\ x_2 \\ \vdots \\ x_{N-1} \end{bmatrix}, \quad \tilde{A} = \begin{bmatrix} I \\ A \\ A^2 \\ \vdots \\ A^{N-1} \end{bmatrix}, \quad \tilde{B} = \begin{bmatrix} 0 & 0 & \cdots & \cdots & 0 \\ B & 0 & \cdots & \cdots & 0 \\ AB & B & 0 & \cdots & 0 \\ \vdots & \ddots & \ddots & \ddots & \vdots \\ A^{N-2}B & A^{N-3}B & \cdots & B & 0 \end{bmatrix}, \quad U = \begin{bmatrix} u_0 \\ u_1 \\ u_2 \\ \vdots \\ u_{N-1} \end{bmatrix}$$

The control horizon m, where $m <= N$. The input command is assumed that $\tilde{u}_k$ changes along control horizon m.

$$\tilde{u}_k = \Delta\ \tilde{u}_k + u_{k-1}$$

$$\tilde{u}_{k+1} = \Delta\ \tilde{u}_{k+1} + u_{k-1} + \Delta\ \tilde{u}_k \qquad (4.14)$$

$$\vdots$$

$$\tilde{u}_{k+m-1} = \Delta\ \tilde{u}_{k+m-1} + \ldots + u_{k-1} + \Delta\ \tilde{u}_{k-1}$$

Merging equations (4.13) and (4.14) then,

$$\tilde{x}_{k+1} = Ax_k + B\,[\Delta\ \tilde{u}_k + u_{k-1}]$$

$$\tilde{x}_{k+2} = A^2x_k + B\,[\Delta\ \tilde{u}_{k+1} + u_{k-1} + \Delta\ \tilde{u}_k] + AB\,[\Delta\ \tilde{u}_k + u_{k-1}]$$

$$\vdots$$

$$\tilde{x}_{k+m} = A^m x_k + (A^{m-1} + \ldots + A + I)B\,\Delta\ \tilde{u}_k + (A^{m-1} + \ldots + A + I)B\,\Delta\ \tilde{u}_{k-1} + (A + I)B\,\Delta\ \tilde{u}_{k+m-1}$$

$$\vdots$$

$$\tilde{x}_{k+N} = A^N x_k + (A^{N-1} + \ldots + A + I)B\,\Delta\ \tilde{u}_k + (A^{N-m} + \ldots + A + I)B\,\Delta\ \tilde{u}_{k+m-1} + (A^{N-1} + \ldots + A + I)B\,\Delta\ \tilde{u}_{k-1} \qquad (4.15)$$

the equation (4.15) can be written as

$$\widetilde{X_k} = \psi\widehat{x_k} + \Upsilon\, u_{k-1} + \theta\, \Delta\, \widetilde{U_k} \tag{4.16}$$

With

$$\widetilde{X_k} = [\widetilde{x_{k+1}} \quad \cdots \quad \widetilde{x_{k+\iota}} \quad \cdots \quad \widetilde{x_{k+m}}]^{\mathrm{T}} \tag{4.17}$$

$$\Delta\widetilde{U_k} = [\Delta\widetilde{u_k} \quad \cdots \quad \widetilde{x_{k+\iota}} \quad \cdots \quad \Delta\widetilde{u_{k+m-1}}]^{\mathrm{T}} \tag{4.18}$$

$$\psi = [A \quad \cdots \quad A^m A^{m+1} \ldots \quad A^p]^{\mathrm{T}} \tag{4.19}$$

$$\Upsilon = \begin{bmatrix} B \\ \vdots \\ \sum_{i=0}^{m-1} A^i B \\ \sum_{i=0}^{m} A^i B \\ \vdots \\ \sum_{i=0}^{p-1} A^i B \end{bmatrix} \tag{4.20}$$

$$\theta = \begin{bmatrix} B & \ldots & 0 \\ AB + B & \cdots & 0 \\ \vdots & & \vdots \\ \sum_{i=0}^{m-1} A^i B & \ddots & B \\ \sum_{i=0}^{m} A^i B & \cdots & AB + B \\ \vdots & \ddots & \vdots \\ \sum_{i=0}^{p-1} A^i B & \cdots & \sum_{i=0}^{p-m} A^i B \end{bmatrix} \tag{4.21}$$

Equations (4.16) is composed of three terms $\theta, \Upsilon,$ and ψ. All the three matrices depend upon the value of A and B and are computed offline. The first two terms represent the free response that depends upon the past and the last term controls the future events or the forced one. The change of controlled input $\Delta\, \widetilde{U_k}$ is computed by minimizing the cost function given by :

$$W_k = \left(\widetilde{Y_k} - \widetilde{F_{d,k}}\right)^T \delta \left(\widetilde{Y_k} - \widetilde{F_{d,k}}\right) + \Delta\widetilde{U_k^T}\ \lambda\, \Delta\widetilde{U_k} \tag{4.22}$$

Where,

$$\widetilde{Y_k} = [C\widetilde{x_{k+1}} \quad \cdots \quad \widetilde{Cx_{k+\iota}} \quad \cdots \quad C\widetilde{x_{k+m}}]^{\mathrm{T}}$$

$$\widetilde{F_{d,k}} = [F_{d,k+1} \quad \cdots \quad F_{d,k+i} \ \cdots F_{d,k+N}]^{\mathrm{T}}$$

The optimal and unique solution $\Delta\widetilde{U_k}$ is therefore equal to

$$\Delta\widetilde{U_k} = (\theta^T \delta\, \theta + \lambda)^{-1} \theta^T \delta\, \widetilde{E_k} \tag{4.23}$$

Where, E_k is the prediction error.

4.6. MPC TUNING

The tracking capability of a system is greatly influenced by the length of the prediction horizon *N*. The computation load increases on the system when the prediction horizon is extended. When the time delay increases in the system, the prediction horizon is extended until having a stable response from the internal plant.

Chapter 5
System Modelling

The work in this chapter focuses on the simulation models that are used to produce the results of the control laws discussed in chapter 4. A 2-R robot is used as a surgical arm at the slave end for the simulation model. Different control strategies are investigated by using Model predictive control suffering from time delay.

5.1. Model for force and position control

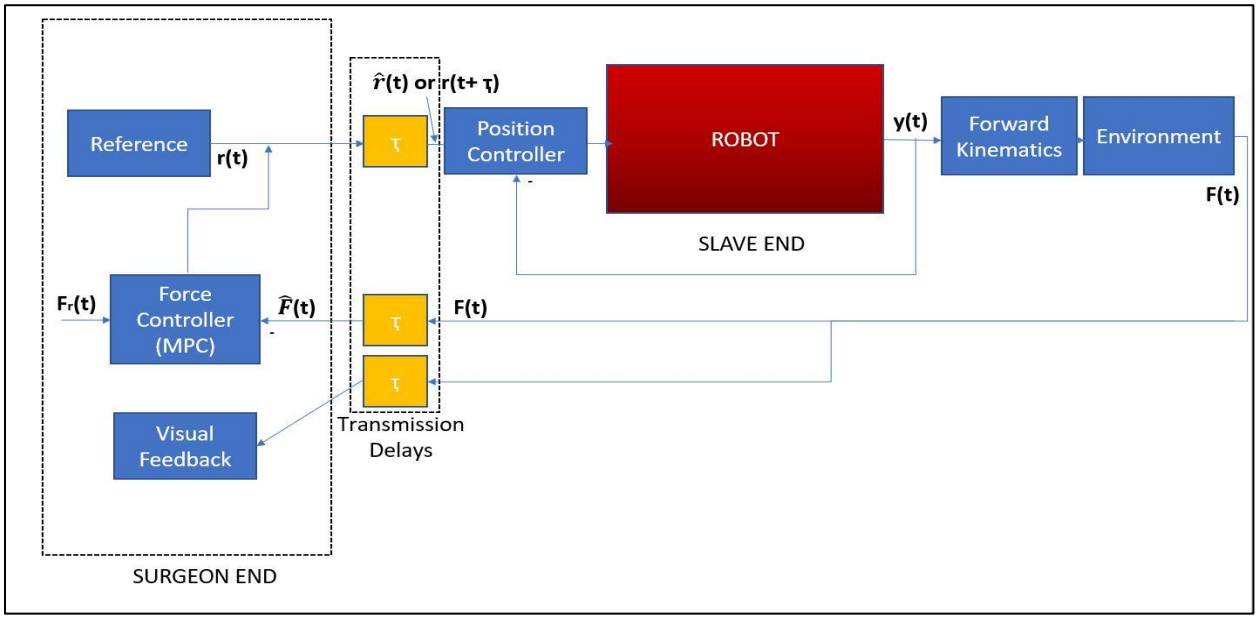

FIGURE 23: MPC AS FORCE CONTROLLER

Figure 24 shows the Simulink model of the hybrid/parallel control using MPC. MPC is used as force control to control the force at the end-effector when meets environment. The system becomes more sensitive in the presence of time delays. The major role of the MPC is to estimate the future

input trajectories such that the system remains stable. MPC as a position controller is described in Figure 25. In this control structure, MPC acts as a regular position controller but if required MPC can be used in such a way that the impact of the end-effector to the environment is minimal. This model will help to prevent the damage to the environment while encountering the situation.

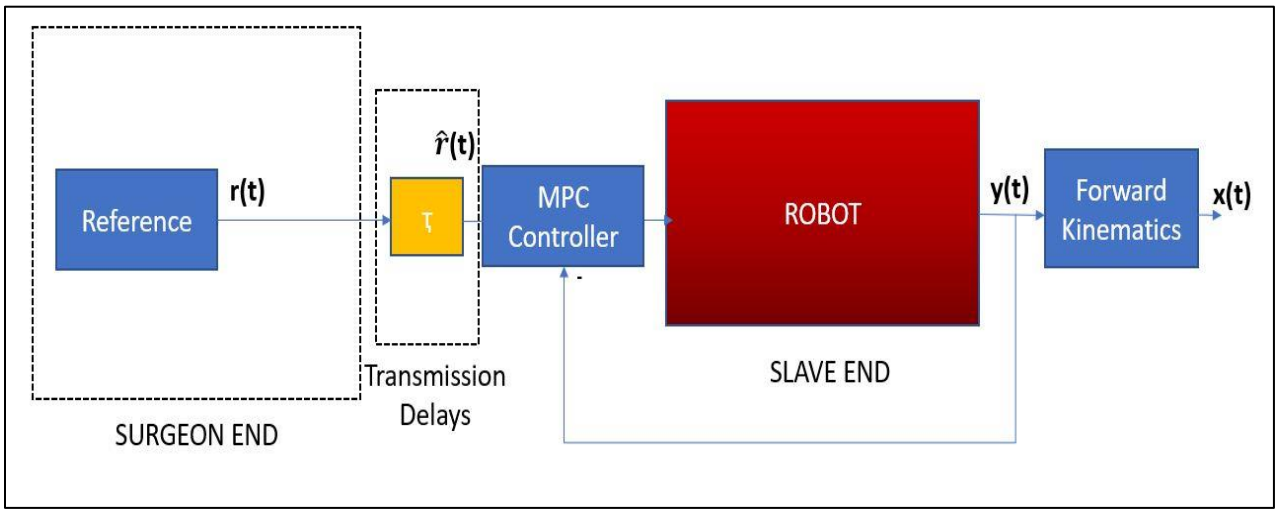

FIGURE 24: MPC AS A POSITION CONTROLLER

5.1.1. Master end

The surgeon at the master end sends input to the slave end after using the visual perception of the operating room. The visual perception helps the surgeon in the decision making of information to the slave end. Many researchers have tried to model the human behavior in the control loop, the Orenstein developed a model close to human behavior taking into neuromuscular effects, but it is comprising of a high number of parameters.

A master model with the simple kinematic model is considered for our system. We have considered that the reference is already known to us to carry out the work for this thesis.

Figure 26. Illustrates the SIMULINK^{TM} model of our system. Master end's control architecture consists of force/position inputs with a localized force controller. For our study, we have used linear MPC to control our system suffering from deterministic time delays.

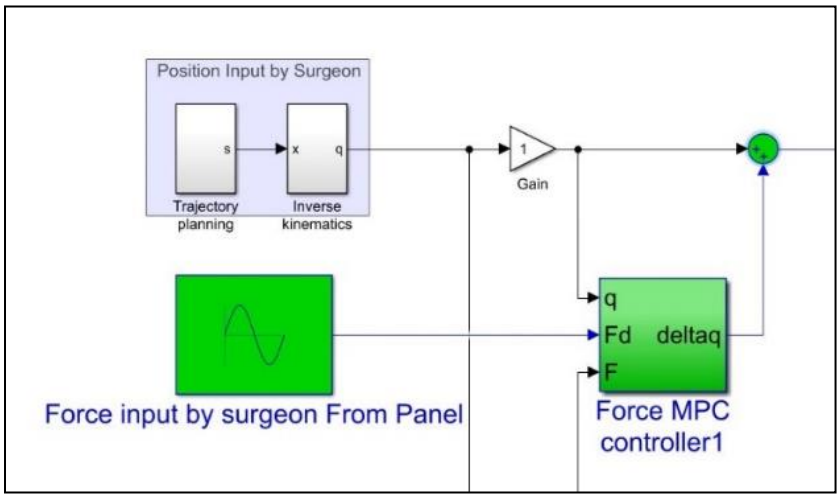

FIGURE 25: A MASTER MODEL OF THE SYSTEM

5.1.2. Slave end modeling

It is essential to know the accurate model of the slave robot with its behavior when it meets the environment. A 2-R DOF manipulator with first order flexible coupling is considered for our system as shown in Figure 27.

The forward kinematic equations of the 2-R robot is given by (5.1), (5.2), (5.3) and (5.4).

$$x_1 = L_1 \sin q_1 \quad (5.1)$$

$$y_1 = L_1 \cos q_1 \quad (5.2)$$

$$x_2 = L_1 \sin q_1 + L_2 \sin (q_1 + q_2) \quad (5.3)$$

$$y_2 = L_1 \cos q_1 + L_2 \cos (q_1 + q_2) \quad (5.4)$$

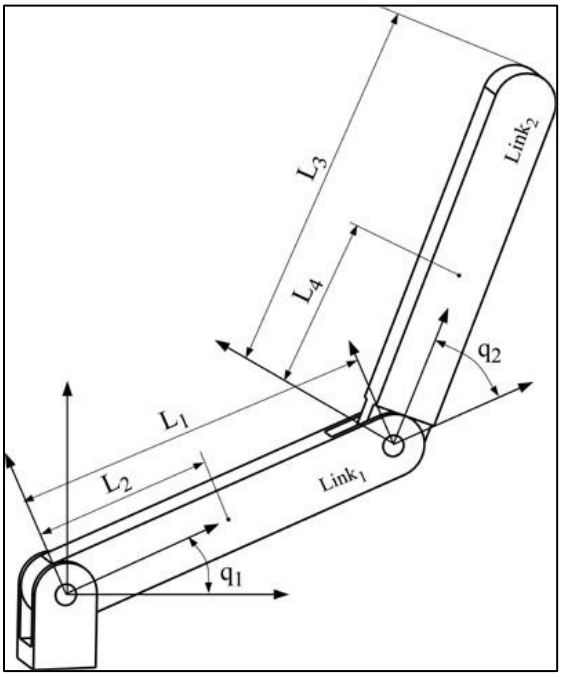

FIGURE 26 : 2-R DOF MANIPULATOR

The dynamic equation of a robot in free space is described by:

$$H(q)\ddot{q} + C(q,\dot{q})\,\dot{q} + g(q,\dot{q}) = T \quad (5.5)$$

Where q, $H(q)\ddot{q}$, $C(q,\dot{q})\,\dot{q}$, $g(\dot{q})q$, and T *are* the angles of joint vectors, the mass/inertia matrix, the Coriolis/centrifugal torque, a gravitational component in joint space and vector of joint torques,

respectively. The dynamics of the robot changes when end-effector meets the environment. The equation *(5.6)* is given by:

$$H(\ddot{q}) + C(\dot{q}, q) + g(q) + J^T f_e = T \qquad (5.6)$$

Where J represents the Jacobian of the end-effector and the vector, f_e, is the contact force at the end-effector. The other robotic parameters such as link length, inertia's, Coriolis components and gravity term are given in Appendix.

Figure 28 shows the dynamic model of our slave robot developed in SIMULINK™. The slave side is equipped with a position controller that is located at the remote site. The position controller gets localized feedback from the robot.

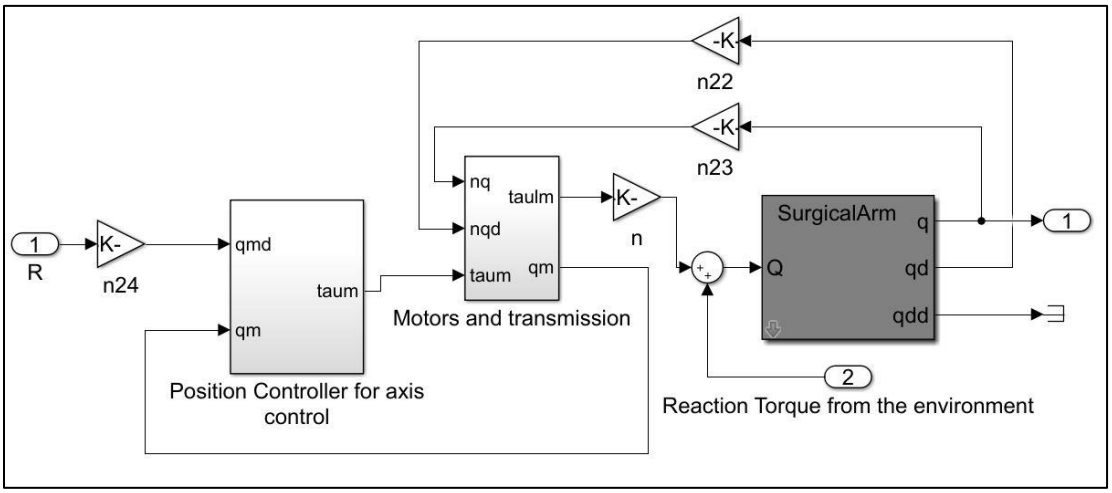

FIGURE 27: SLAVE MODEL FOR THE SURGICAL ARM

The reaction that acts on the robot when in contact with the environment is calculated in the form of reaction torque and is added as feedforward disturbance to the input torque of the manipulator.

The feedback from the robot in the form of angular velocity, angular position is provided to the controllers that send commanded input to the actuators. The actuators are fitted with artificial flexible coupling with localized feedback.

5.1.2.1. Environment modeling

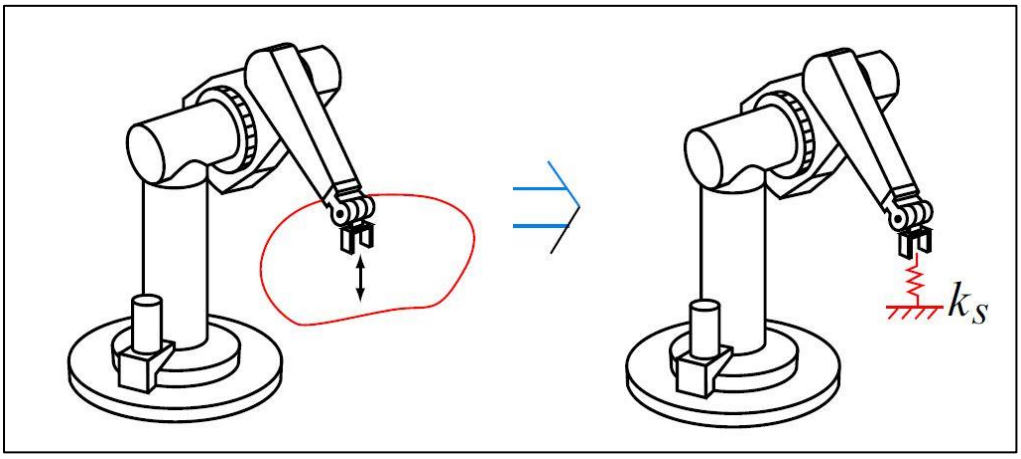

FIGURE 28: MODEL OF THE CONTACT ENVIRONMENT [84].

It is essential to find a relation between the contact force and the motion of the end-effector in the force control direction. It is very hard in practice to find an exact model of the environment of contact. A simple spring model can be used for the design of a controller as shown in Figure 29. We have assumed a constant stiffness of 10000 kPa is assumed for our thesis. As per the Figure 17. A human bone has a stiffness around in the range of 10000 kPa.

Human body comprises various tissues whose stiffness varies from 1 kPa to 20,000 kPa. Therefore, the surgical system should have an ability to estimate the contact stiffness accurately when meeting the environment. The spring model is too simple, but it captures the vital characteristic that contact force on most passive objects increases with deflection.

$$F_e = K_e*(x - x_e) \tag{5.7}$$

A higher order model for the environment consists of mass and damping factors along with stiffness of the system. Adding a mass to the simple spring model reduces the performance of the system. Hence, a simple spring model is an excellent conservative model regarding stability. So, the proposed model of spring is used to design the controller for our thesis.

5.1.1. Communication channel

Simulations for the proposed control law are carried out in MATLAB™ SIMULINK toolbox. Bi-lateral communication system consists of 2-time delays as shown in Figure 30 between the master and slave end. The communication delays are introduced into the system using time delay blocks in Simulink as shown in Figure 28. The time delays are assumed deterministic and known that has to be relaxed in future.

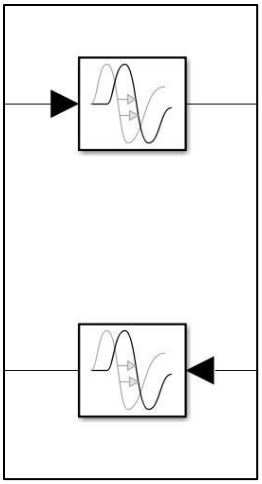

FIGURE 29: TIME DELAY'S IN BI-LATERAL OPERATION

Time delays are approximated by using padé approximation of 3rd order to approximate the time delays in the process.

5.2. Kinematic Predictive Imaging modeling

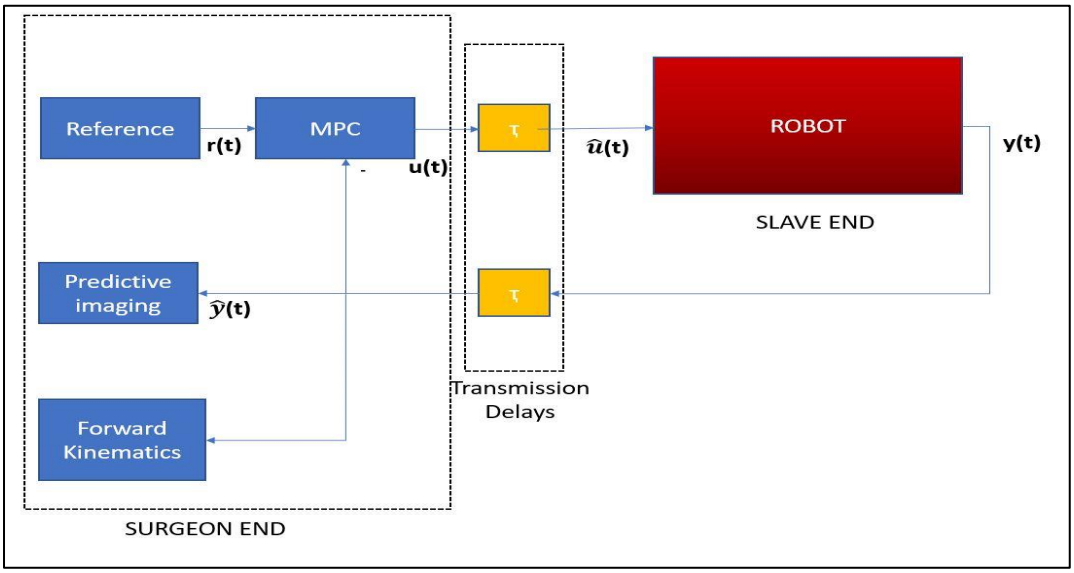

FIGURE 30: KINEMATIC PREDICTIVE IMAGING

This part of the chapter discusses the Simulink model used to show the effectiveness of the control law to produce predictive imaging at the master end.

MPC is used as a position controller at the local site rather than the remote site as discussed in chapter 4. MPC produces predicted output in the form of joint coordinates that is used to create a line animation of the slave robot on the master console. Petercorke™ robotics toolbox for MATLAB™ is used to generate the line animation of the 2-R robot.

The robot's parameters are the same as explained for the force/position control law. MPC ability to investigate the future of the model helps to control the time delayed system. The communication delay used to study the control law is 70ms that remains constant throughout the process. The control structure of the kinematic predictive imaging is given in Figure 31.

Chapter 6
Simulation Results and Discussions

The proposed control algorithms for the teleoperation discussed in the previous chapters are evaluated through simulation results.

A 2-DOF manipulator is considered to demonstrate the effectiveness of the above-discussed algorithms. The dynamics of the master end, slave end, and the environment are discussed in the chapter-4. It is assumed for the simulation results that the end-effector makes point contact with the environment.

System Parameters:

L_1 = 1 m is the length of the link 1.

L_2 = 1 m is the length of the link 2.

M_1 = 50 kg, the mass of the link 1.

M_2 = 50 kg, the mass of the link 2.

θ_1 is the rotational angle of the joint 1.

θ_2 is the rotational angle of the joint 2.

$Lc_1 = Lc_2$ = 0.5m is the length to the mass centre of the link.

K_e =1. e+7 [N/m], Stiffness of the environment for the hard tissue.

y_e = 2.82.e-5 [m], Environnent position.

All the values are expressed in metric units.

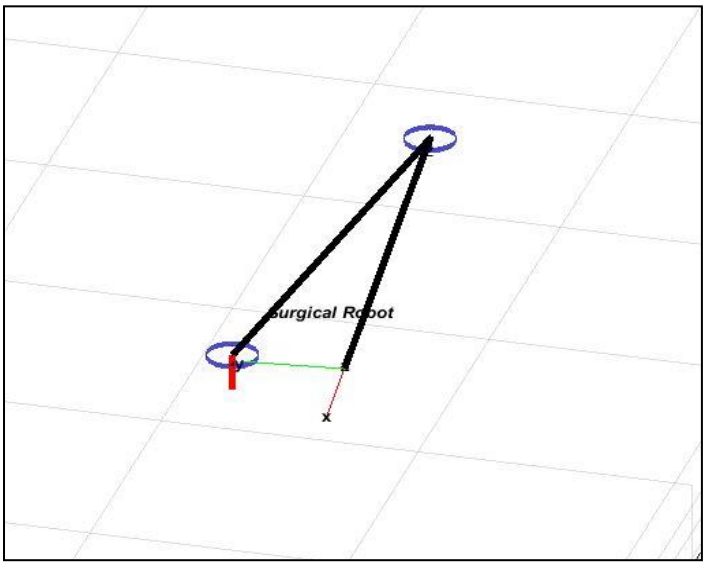

FIGURE 31: SURGICAL ARM WITH 2 DOF

Denavit - Hartenburg representation for the 2-R robot is shown above in Figure 32 in Table 6.1 below:

TABLE 6.1: D-H PARAMETERS OF THE 2-R ROBOT

Joint no.	a_i	α_i	d_i	θ_i
1.	L_1	0	0	θ_1
2.	L_2	0	0	θ_2

Table 6.2 shows the dynamic parameter of the actuators considered to carry out the simulation [89].

TABLE 6.2: DYNAMIC PARAMETERS OF THE MANIPULATOR

Sr. No	Parameters	Values
1.	Moment of inertia of the motors(Jm_1)	5.e-3 $kg.m^2$
2.	Moment of inertia of the motors(Jm_2)	2.e-3 $kg.m^2$
3.	Stiffness for coupling (Kel_1)	70 Nm^{-1}
4.	Stiffness for coupling (Kel_2)	70 Nm^{-1}

5.	Viscous damping (del_1)	0.05 Nsm^{-1}
6.	Viscous damping (del_2)	0.05 Nsm^{-1}
7.	Reduction ratio (n)	100

Table 6.3 shows the initial condition of the actuators, end-effector and link positions.

TABLE 6. 3: INITIAL CONDITIONS OF THE ARM

Sr. No	**Parameter**	**Initial condition**
1.	Initial motor position (qm_0)	[-147.06,294.12] rad
2.	End of effector position	[0.2,0] m
3.	Initial link position (q_0)	[-1.47,2.94] rad

6.1. Force Control using MPC

The proposed control scheme for the MPC is discussed in chapter 4 apply to the above discussed surgical system. The controller is implemented on the master side. Two different scenarios are considered during implementation that is as follows:

1. Reference Known: - This is the case when the MPC already know the reference and previewing of the reference is done to compensate for the time delay and its effects. This is the scenario in the Surgical Arms capable of operating in autonomous mode.

2. Reference Unknown: - In the shared controlled surgical arms controller does not know the reference beforehand. As a result latency cannot be compensated. The prime objective of the controller, in this case, is to compensate for the effects of time delay.

The robot will be tested with different constant time delays as suggested in Table 2.1. The environment is known and frictionless such that robot is applying force on the negative y-direction while moving parallel to the x-axis for 30 cm with trapezoidal velocity profile with a maximum velocity of 3 mm/s in 15 seconds as shown in Figure 33. Initially, the robot is not in contact with the environment and comes in contact when y coordinate is 2.82.e-5 m.

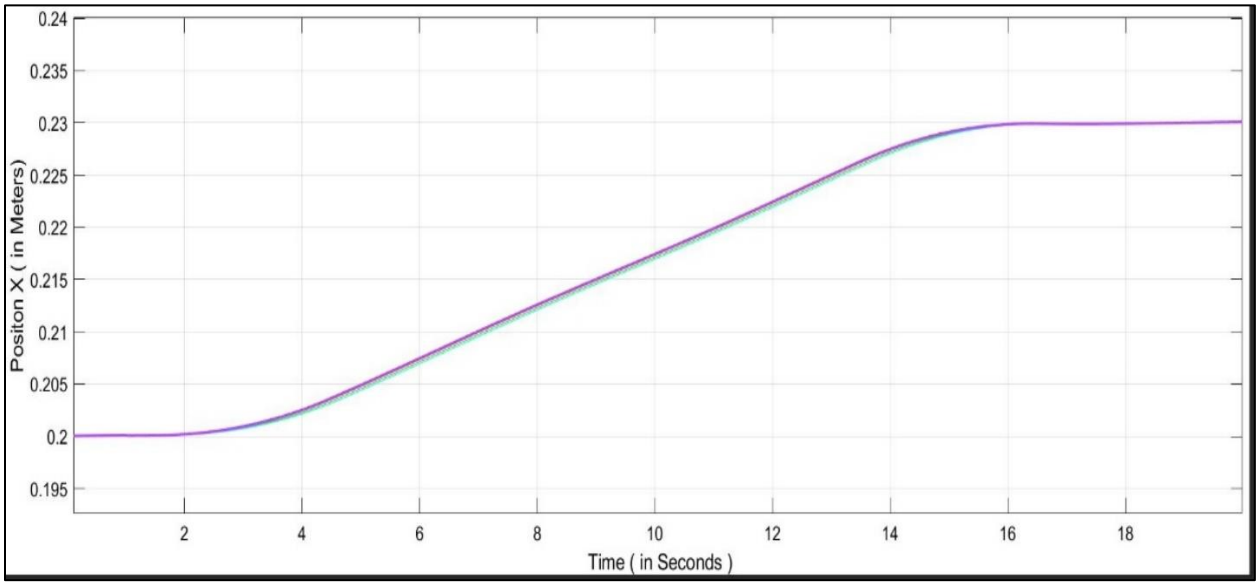

FIGURE 32: POSITION OF THE ROBOT IN X PLANE W.R.T TIME

Figure 34 illustrates that with the increase in the dead time, the transient response duration in the system increases and it can be controlled by tuning the weights of MPC to get an overshoot free system. The response of the system gets slower as the weight's are made less aggressive with the increase of time delay. Overshoot of less than 10% was observed with the time delay of 100ms when using MPC for specific tuning weights of MPC with no time delay are used.

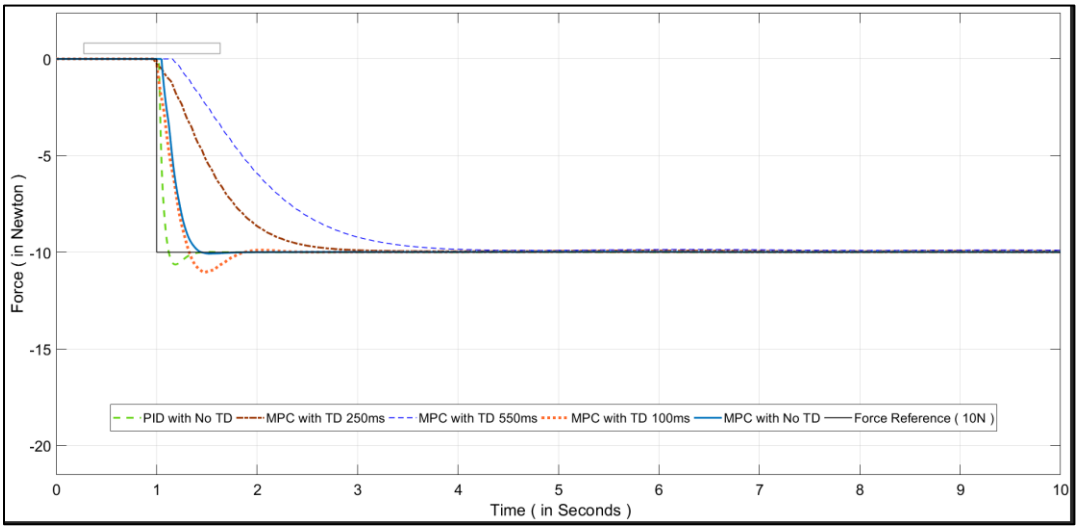

FIGURE 33: FORCE CONTROL USING MPC (WITH PREVIEWING) WITH A DIFFERENT TIME DELAYS WITH 10^7 N/M STIFFNESS

Figure 35 shows that previewing can help compensating the effect of dead time in the system as we can see that MPC is prepared for the dead time ahead of its time. All the responses with different time delays are tuned for previewing in such a way that makes their response close to the reference of the system showing no or minimal dead time effect on the response of the force control.

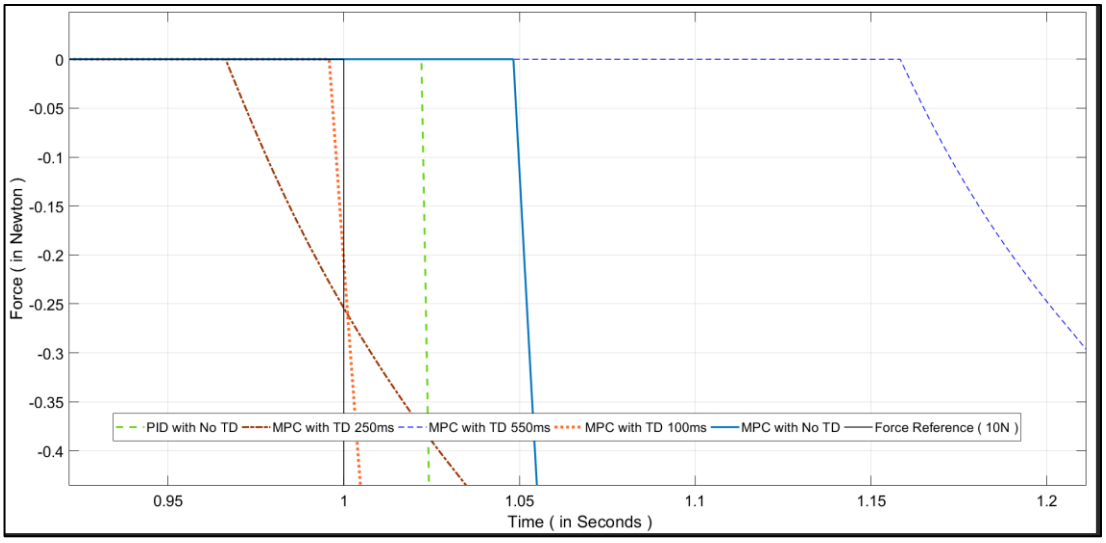

FIGURE 34: ZOOMED VIEW OF THE FIGURE 5.3 AROUND TIME STAMP 1 SECOND WHEN FORCE STARTS ACTING ON THE SYSTEM.

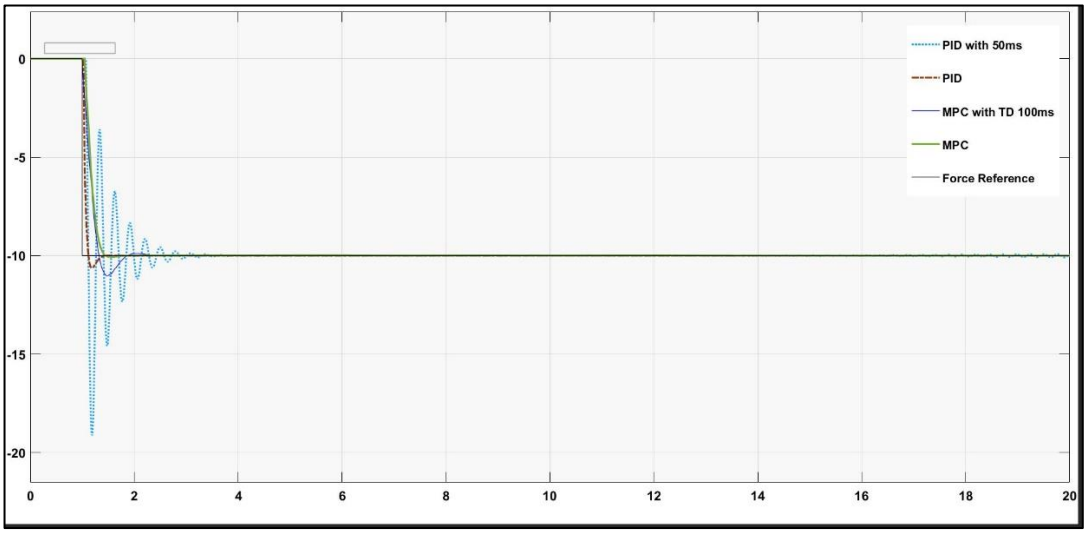

FIGURE 35: COMPARISON OF MPC VS PID WITH TIME DELAY

Figure 36 presents a comparison of PID controller vs MPC with time delay. PID results in a highly oscillatory response with the time delay of 100ms and hence making the system unstable. Hence, the time delay of 50ms is considered for PID to compare with MPC with dead time 100ms. The

system's response with PID is oscillatory and cannot be damped by changing the tuning parameters. MPC has shown its robustness as compared to PID with double the time delay.

Figure 37 shows the position of the surgical arm in the Y plane versus time. It compares the type of contact robot is making in the presence of time delays with MPC and PID controllers. PID with the time delay shows unstable contact with the environment versus stable contact by MPC under different time delays.

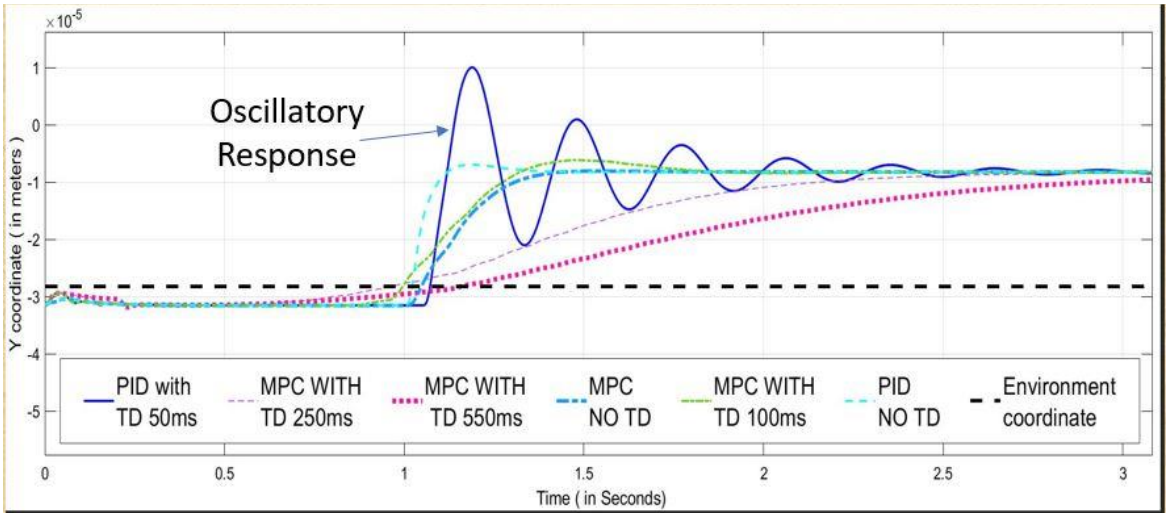

FIGURE 36: POSITION OF THE ROBOT IN Y PLANE VS TIME

In the situation when the reference is not available to the MPC, i.e. no previewing, the dead time cannot be compensated in that situation. The effects of dead time are neutralized by the MPC unlike PID as shown in Figure 38. The simulation results indicate that the system is stable under the control of MPC.

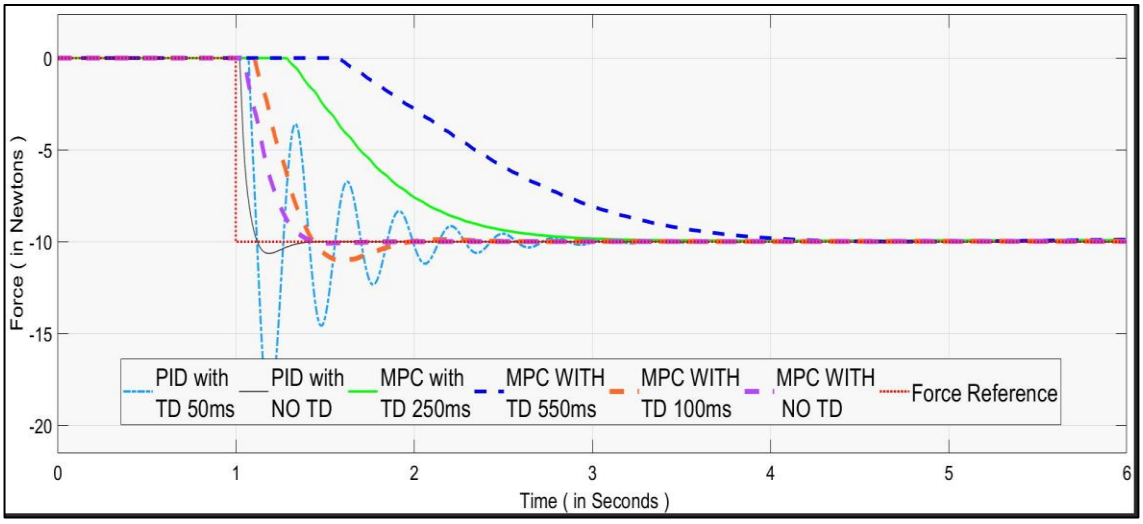

FIGURE 37: MPC VS PID WITH DIFFERENT TIME DELAYS WITH NO PREVIEWING

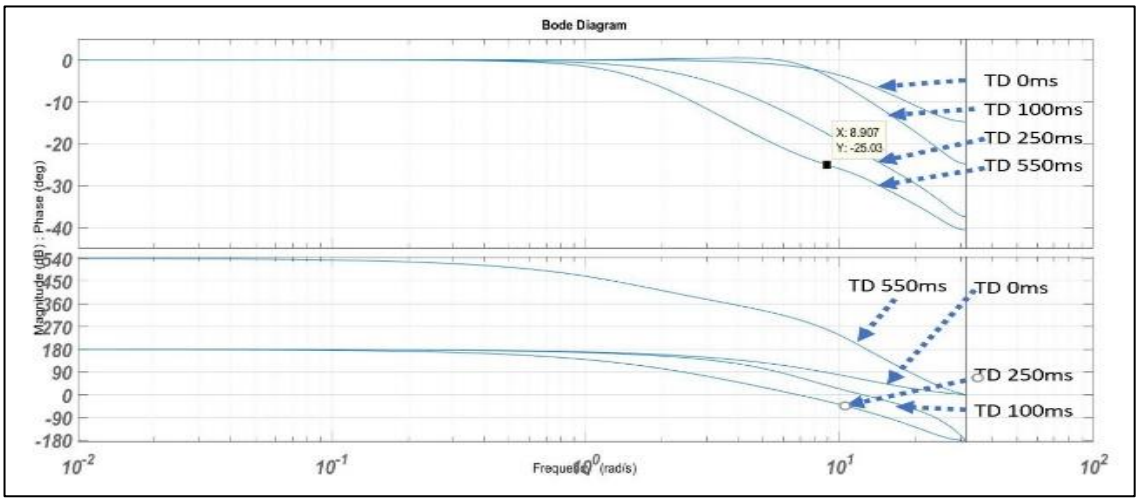

FIGURE 38: BODE PLOT FOR THE SYSTEM UNDER DIFFERENT TIME DELAYS

Figure 39 shows the frequency analysis of the system with different time delays by using Bode plot. The phase lag increases with the increase of the time delay as described in the above figure with an increase of frequency. The time delays considered in the system are approximated by using the Padé approximation technique. Increasing the frequency of the system increases the

computational load on the system increases demanding for more computation power. But, since the system gets the linearized system is controllable even when the frequency is increased.

Table 6.4 shows the control parameters for different time delays for the model predictive force control of the robot. The sampling interval has been kept to 100 ms throughout the simulation for the force control. When the time delay increases the controller tends to go unstable if not tuned to handle the different time delays. An important observation is made as shown in Figure 34 that if no delay condition's tuning parameters are used for a time delay of 100 ms, an overshoot of less than 10% is observed. Overshoot less than 10% is acceptable with time delay is acceptable for the process.

MPC can control the overshooting in the process by changing the control parameters. The overshooting in the process is controlled by increasing the rate of change of manipulated variable i.e. by making the weights less aggressive. Systems response gets slower when the weights are increased on the system as shown in Table 6.4.

The prediction horizon of the system is increased when the time delay increases such that the MPC can investigate the future more to handle the delayed system in a better way. Increasing the prediction horizon increasing the computation load on the system.

TABLE 6.4: CONTROL PARAMETERS FOR MPC AS A FORCE CONTROL WITH TIME DELAY

Sr.No.	Control Parameters	0 ms	100 ms	250 ms	550 ms
1.	Sampling time (k) (in ms)	0.1	0.1	0.1	0.1
2.	Prediction Horizon (p)	35	120	150	200
3.	Control Horizon (m)	5	20	20	20
4.	Input scale factors (s_u)	1	1	1	1
5.	Output scale factors(s_y)	1	1	1	1
6.	Weight on Manipulated variable (w_u)	0	0	0	0
7.	Weight on Rate of change of Manipulated variable (w_{du})	0.0246596963941606	0.122140275816017	0.222554092849247	4.94261860528944
8.	Weight on Manipulated output (w_y)	4.05519996684468	9.0060382838578	4.94261860528944	3.31313633103422

6.2. Impact Modelling using MPC

In this section of the chapter, the results by using control law discussed in chapter 4 by using MPC as a position controller are discussed. MPC as a position control is used at the remote side. It acts as a localized controller at the slave end. The primary objective of this control law is to minimize the impact on the environment and the end of effector to avoid the damage to the environment.

The robot will be tested with constant round-trip time delay equivalent to 70 ms. It is assumed that the reference is available to the MPC for previewing. This application is useful for the surgical arms having the capability to work on autonomous mode under the supervision of the surgeon.

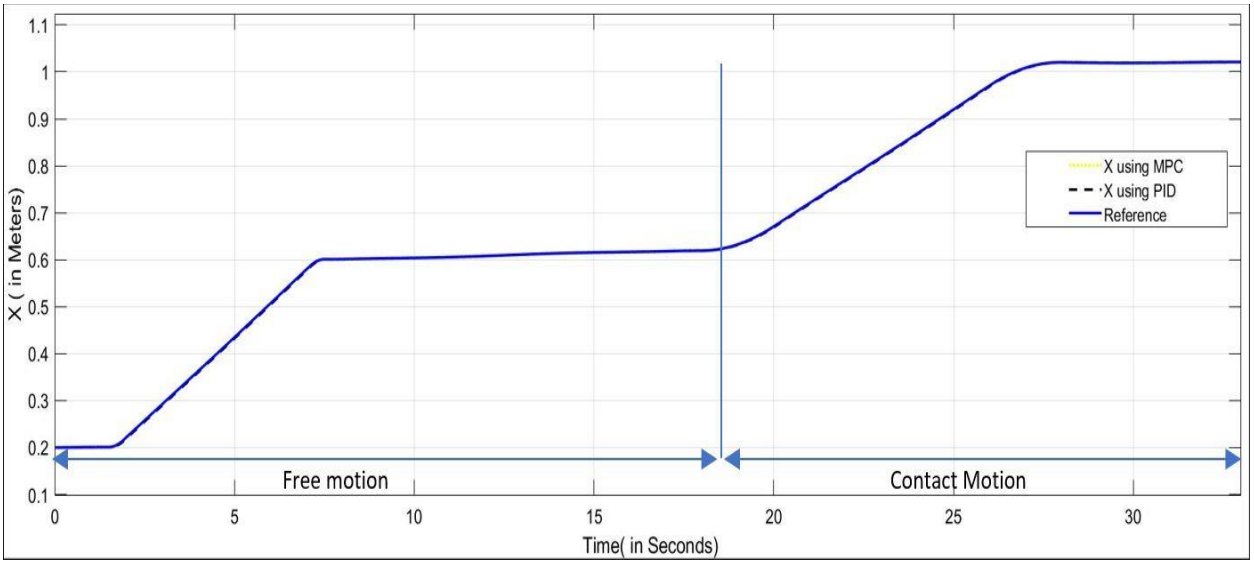

FIGURE 39: POSITION OF THE ROBOT IN X-PLANE W.R.T TIME

Figure 40 illustrates the slave robots free and in contact motion in the X-plane w.r.t time. Robot contacts the environment when the X = .63 m. As described in the Figure 41 the robot moves with the trapezoidal velocity profile to move a smooth transition with a maximum velocity of 70 mm/s. The reference is designed in such a way that the robot slows down as it reaches close to

the contact point. A maximum of speed of 10 mm/s is recommended for the process of minimum invasive surgery.

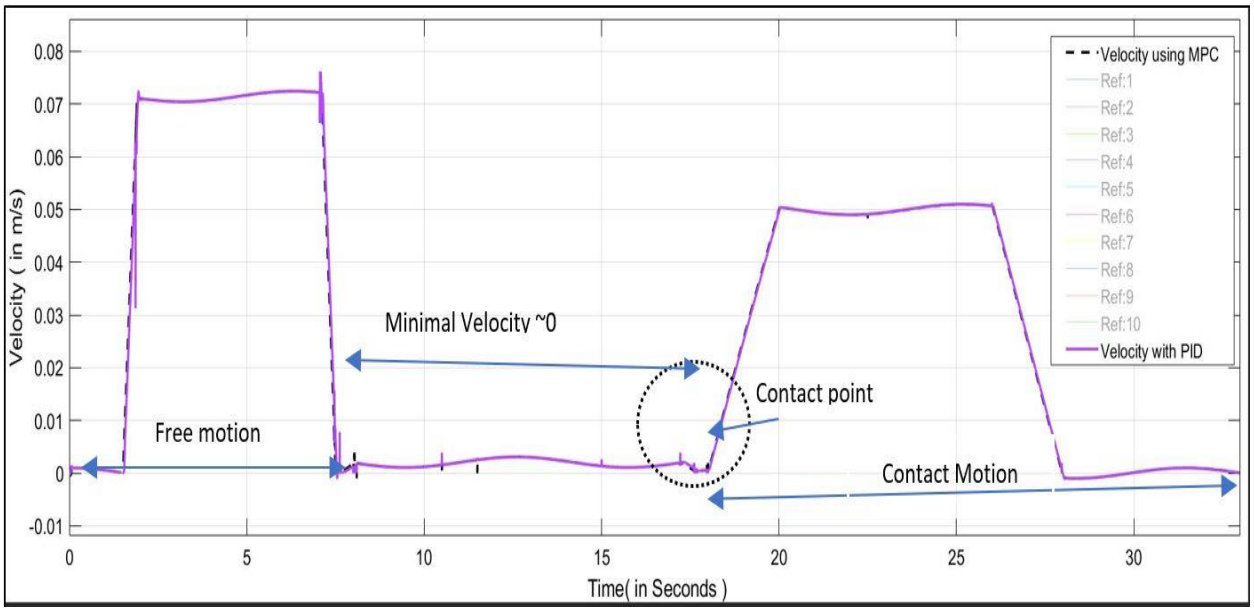

FIGURE 40: TRAPEZOIDAL VELOCITY PROFILE OF THE ROBOT USING PID VS. MPC W.R.T TIME

The reference is designed in a way such that the robot slows down when it reaches close to the contact point. Figure 42 shows a comparison of the velocity profiles by using PID and MPC as a position controller. The graph shows a stable response from the system with a time delay with both the controllers. Since the time delay is in the input of the position controller, it does not affect the control performance of the system. A latency equivalent to the delay length is observed in the system.

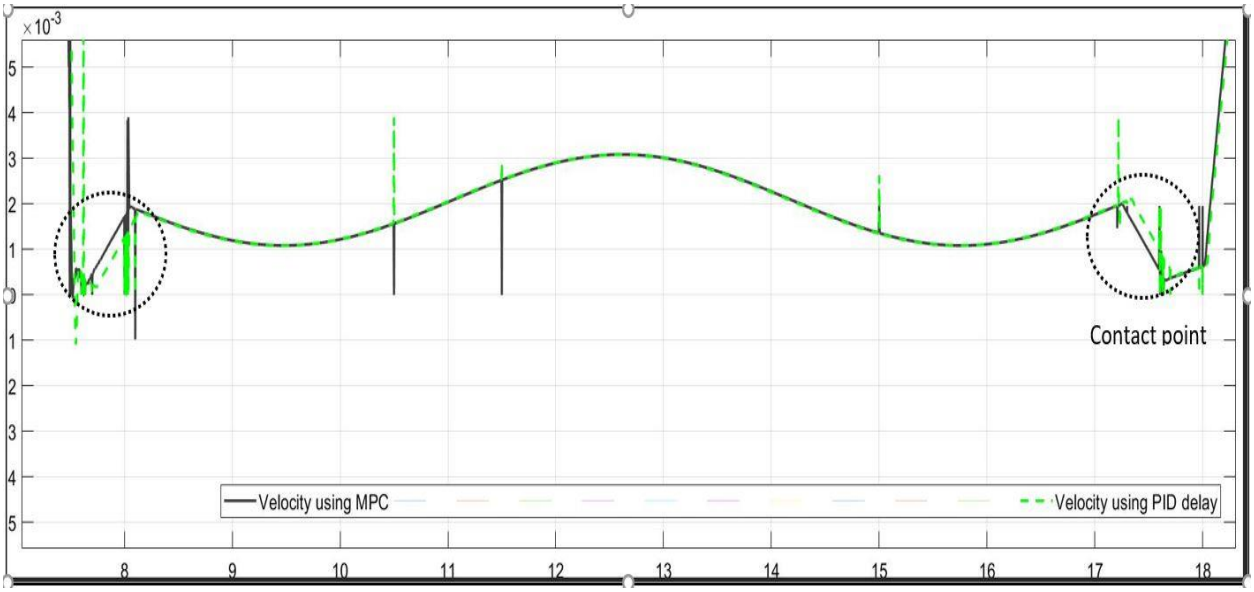

FIGURE 41: PANNED VIEW OF FIGURE 5.10 TO SHOW THE CONTACT

Figure 42 shows how MPC predicts the future velocity of the system by looking a few steps ahead at this moment reaches the velocity of contact point few steps ahead than PID as shown above. In other words, MPC used previewing of the reference to compensate for the time delay in the system, and by selecting appropriate previewing steps, it can generate the control inputs ahead of its time to reach to the desired point. This feature of MPC is helpful to attain a velocity result in a minimum impact on the environment, unlike PID. PID lacks in ability to preview and compensate the latency in the system.

Table 6.5 shows the control parameters of the MPC used to control the impact on the environment. Since the position control is located at the remote site, it only suffers from input delay. The feedback to the master end from the slave end is in the form of force feedback or visual feedback with delay. A delay of 35 ms is considered as the input delay for the process.

TABLE 6.5: CONTROL PARAMETERS FOR MPC AS A POSITION CONTROL WITH TIME DELAY FOR MINIMUM IMPACT VELOCITY

Sr. No.	Control Parameters	35 ms (70 ms round trip)
1.	Sampling time (k) (in ms)	0.01
2.	Prediction Horizon (p)	100
3.	Control Horizon (m)	35
4.	Input scale factors (s_u)	1
5.	Output scale factors(s_y)	1
6.	Weight on a Manipulated variable (w_u)	0
7.	Weight on Rate of change of Manipulated variable (w_{du})	[0.09,.001]
8.	Weight on Manipulated output (w_y)	[25,30]

6.3. Kinematic Predictive Imaging using MPC

The last section of the chapter focuses on the kinematic predictive imaging by exploiting the control law developed using MPC. MPC is used at the master end with the idea to generate a synthetic image which compensates the delays in the loop and predict future end effector positions such that the surgeon sees an image without delay.

The robot will be tested with a constant round-trip time delay equivalent to 70ms. The assumptions are like that of minimum impact velocity such that the reference is available to the MPC for previewing. This application is useful for the surgical arms having the capability to work in autonomous mode under the supervision of the surgeon. To develop a delayed free perception Peter Corke's robotic toolbox is used.

The robot is commanded to move along the x-axis until it reaches a steady state after 15 seconds. The system has a round trip delay of about 70ms. The control law developed using MPC in chapter 4 is used to create a simple delayed free simulation of the slave end.

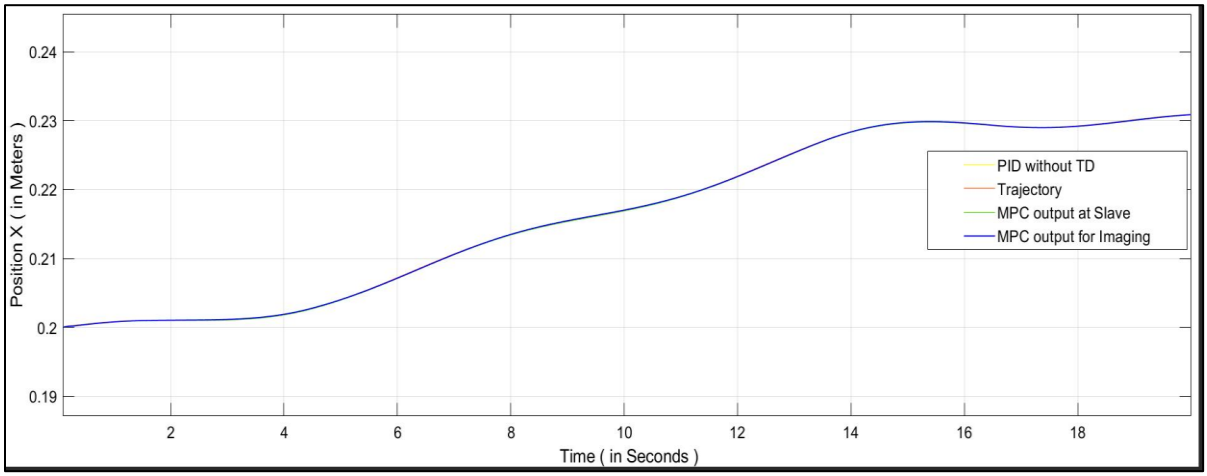

FIGURE 42: COMPARISON OF ROBOTIC MOTION ABOUT X-AXIS W.R.T TIME USING MPC AND PID

Figure 43 compares the position control of the 2-R DOF system with the MPC and PID as position controller. The perception at the master end is close to the output at the operating room.

MPC used previewing to predict in such a way such that the output at the master end and the slave end at a time instant are close. The output at the master end from the MPC to develop line animation of the robot working in an operating room that can be further developed with a CAD model of the slave end.

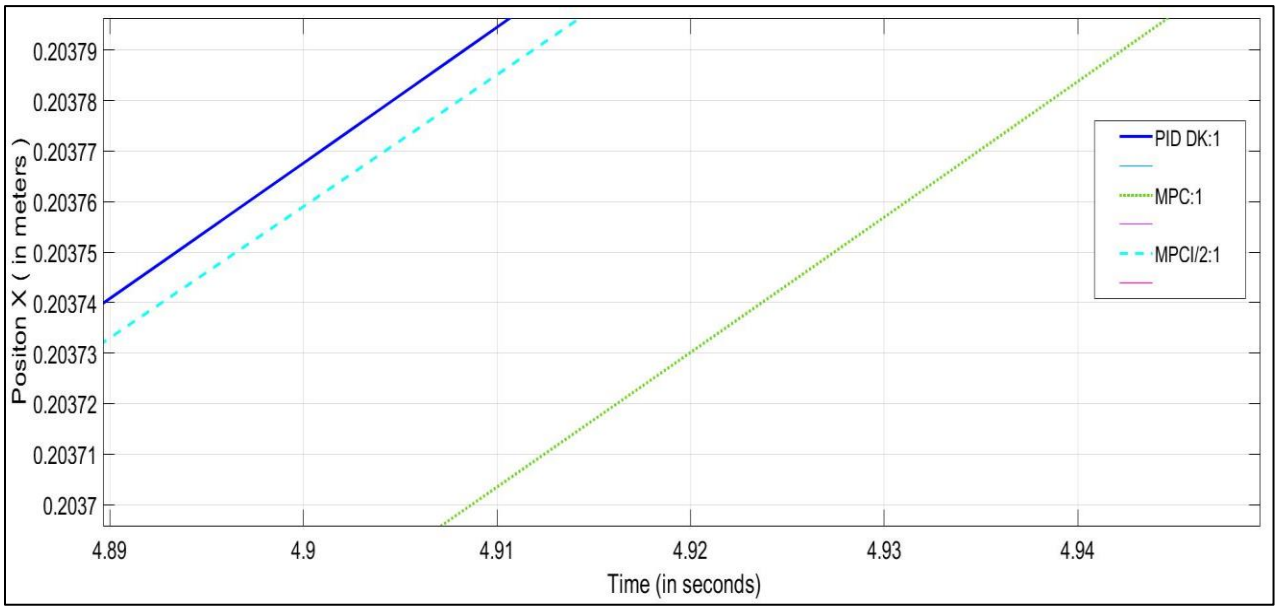

FIGURE 43: COMPARISON OF THE ACCURACY OF THE ROBOT W.R.T TIME USING MPC AND PID

Figure 44 shows the accuracy of the prediction between the master side and slave end. The prediction provided by the MPC is just 5ms behind the reference signal which is undetected by the humans otherwise in the present commercial system it takes delay equivalent to the length 35ms

to reach to the master console. In other words, the surgeon can now get some delayed free information about the operating room. From the simple line animation shown in the Figure, 45 surgeon can at least determine the type of contact of the robot with the environment until receiving real-time perception.

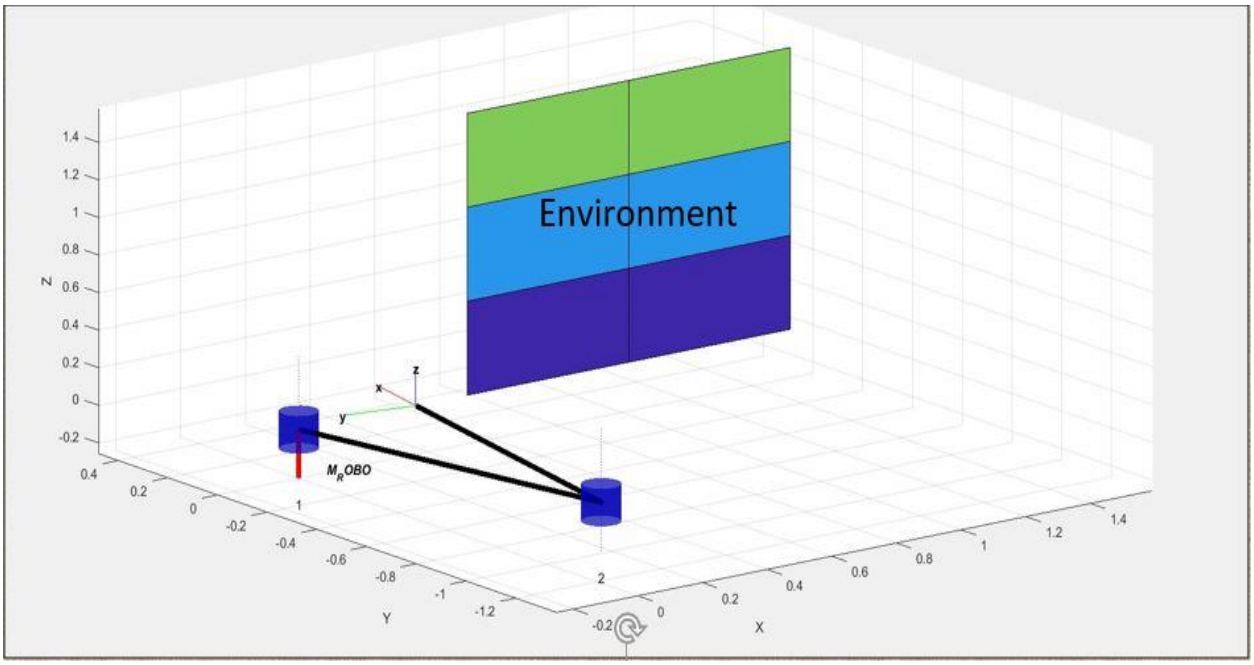

FIGURE 44: KINEMATIC PREDICTIVE IMAGING

Figure 45 shows the delayed free predictive imaging developed to give delayed free perception to the surgeon of the operating room. Later this imaging can be further improved by using actual CAD model of the robot with the information of the environment to give better information to the surgeon.

Table 6.6 is the measures of control for the system. A round trip delay of 70ms is considered for the testing of the system.

TABLE 6.5: CONTROL PARAMETERS FOR MPC TO GENERATE KINEMATIC PREDICTIVE IMAGING WITH TIME DELAY

Sr. No.	Control Parameters	70 ms
1.	Sampling time (k) (in ms)	0.01
2.	Prediction Horizon (p)	165
3.	Control Horizon (m)	85
4.	Input scale factors (s_u)	1
5.	Weight on Manipulated output (w_y)	[6,3]
6.	Output scale factors(s_y)	1
7.	Weight on Manipulated variable (w_u)	0
8.	Weight on Rate of change of Manipulated variable (w_{du})	[0.1,0.1]

Chapter 7
Future Work

Since most of the robots used in the medical field are having more than 2-DOF, it is essential to test the above-shown control laws formulated for those robots like da Vinci Surgical System, RAVEN and many others are in the field of the medical robots, so that the work gets extended to the above-mentioned manipulators.

Delays and packet losses on the internet vary with the time showing a random behavior in real-time applications. Therefore, it is mandatory to test the control laws for time-varying delays which will also focus our future work with experimentation work. Gain scheduling using MPC can be done to handle the time-varying delays. Such kind of work is expected to show more a considerable difference in the performance of MPC over PID.

Chapter 8
Conclusions

The control laws developed in this thesis were validated for the 2-DOF slave robot. Force control laws developed with a different set of time delays were tested on the model and showed the effectiveness of the MPC as a force controller over PID. The system suffers from overshooting if not designed for time delays, and the overshooting in the systems response can be reduced by using MPC.

Force control strategy developed was tested under the different set of time delays. It was observed that with the increase of the time delay the response of the system gets slower using MPC, but no overshooting was observed. The comparison of the time delayed system controlled with MPC was done PID controlled system. PID shows significant oscillatory response when the time delay is more than 50ms. It is also shown in the results that time delay could be compensated when reference is known by using MPC's previewing feature. This feature allows the master and slave end work in synchronization practically without any latency.

MPC when used as a position controller, the results show its ability to investigate the future to attain minimum velocity before the impact with the environment, unlike PID. This model will help the surgical arms with the ability to perform autonomously to achieve minimal impact while interacting with the environment. Hence, the damage to the tissue due to impact of the robot with the environment can be prevented.

Kinematic Predictive Imaging using MPC is a novel approach developed to help the surgeons to have a practically delay-free perception of the operating area. This approach can overcome the limitation that the present surgical systems have due to the delayed understanding of the environment.

REFERENCES

[1] Hanly, Eric J., and Timothy J. Broderick. "Telerobotic surgery." Operative techniques in general surgery 7, no. 4 (2005): 170-181.

[2] M.-T. Huang, P.-L. Wei, C.-C. Wu, I.-R. Lai, R. J. Chen, and W.-J. Lee, "Needle scopic, laparoscopic, and open appendectomy: A comparative study," Surgical Laparoscopy, Endoscopy & Percutaneous Techniques, vol. 11, no. 5, pp. 306–312, Oct. 2001.

[3] S. Sauerland, R. Lefering, and E. Neugebauer, "Laparoscopic versus open surgery for suspected appendicitis," Cochrane Database of Systematic Reviews, vol. 4, p.Art. No.: CD001546, 2002, DOI: 10.1002/14651858.CD001546.pub2.

[4] C.Wullstein, M. Golling, and W. O. Bechstein, "Telerobotics in laparoscopic general surgery," European Journal of Surgery, vol. 36, no. 4, pp. 233–238, 2004.

[5] U. A. Hagn, "The Aspect of Versatility in the Design of a Lightweight Robot for Surgical Applications," Ph.D. dissertation, University of Hannover, 2011, ISBN: 978-3-86853-797-0.

[6] C. Wagner, N. Stylopoulos, and R. Howe. The role of force feedback in surgery: "Analysis of blunt dissection". In Proc. of the 10th Annual Haptics Symposium, March 2002.

[7] Y. Tipsuwan and M.-Y. Chow. "Control methodologies in networked control systems". Proceedings of the IEEE, vol. 11, no. 10, pages 1099–1111, 2003.

[8] S. Zampieri. "Trends in networked control systems". In 2008 IFAC World Congress, pages 2886–2894, Seoul, Korea, July 2008.

[9] A.Ainchwar, J.S.Ladoiye and D.Necsulescu, "Analysis of Wireless and Internet Link Failure Effects on Open Loop Remote Control of Motors" , ALLSENSORS 2018, Rome, Italy, pages 49-53, ISBN: 978-1-61208-621-7.

[10] E. Schippers and V. Schumpelick. *Computer-Integrated Surgery*, "chapter Requirements and Possibilities of Computer-Assisted Endoscopic Surgery", pages 561–565. MIT Press, 1995.

[11] B. Davies, S. Starkie, S.J. Harris, E. Agterhuis, V. Paul, and L.M. Auer. Neurobot: "A special-purpose robot for neurosurgery". In *Proceedings of the 2000 IEEE International Conference on Robotics and Automation*, 2000.

[12] V.F. Munoz, C. Vara-Thorbeck, J.G. DeGabriel, J.F. Lozano, E. Sanchez-Badajoz, A.Garcia-Cerezo, R. Toscano, and A. Jiminez-Garrido. "A medical robotic assistant for minimally

invasive surgery". In *Proceedings of the 2000 IEEE International Conference on Robotics and Automation*,2000.

[13] Jonathan M. Sackier and Yulun Wang."Computer-Integrated Surgery", chapter Robotically Assisted Laparoscopic Surgery: From Concept to Development, pages 577–580. MIT Press, 1995.

[14] Armstrong Healthcare Inc. http://www.armstrong-healthcare.com/, December 2001.

[15] M. C. Cavusoglu, F. Tendick, M. Cohn, and S. Sastry." A laparoscopic telesurgical workstation". IEEE Transactions on Robotics and Automation, 1999.

[16] D.S. Kwon, K.Y. Woo, S.K. Song, W.S. Kim, and H.S. Cho. "Microsurgical telerobot system". In Proceedings of the IEEE/RSJ Int. Conf. on Intelligent Robots and Control Systems, 1998.

[17] KAIST. http://robot.kaist.ac.kr/research/main/telesurgery.html, April 2002.

[18] Institut für angewandte Informatik ARTEMIS, Forschungszentrum Karlsruhe. http://wwwserv2.iai.fzk.de/~artemis, December 2001.

[19] M. Ghodousssi, S. Butner, and Y.Wang, "Robotic Surgery – The Transatlantic Case," in ICRA - Proc. of the IEEE Int. Conf. on Robotics and Automation, 2002.

[20] Intuitive Surgical, "Company profile of Intuitive Surgical, Inc., Sunnyvale, CA,USA," Website, 06 2011, [Link accessed 13-August 2011]. [Online]. Available: http: //www .intuitivesurgical.com

[21] Institute of Robotics and Mechatronics. (2010). "MIRO / KineMedic". Retrieved April 2011, from http://www.dlr.de/rm-neu/en/desktopdefault.aspx/.

[22] Institute of Robotics and Mechatronics. (2010). "MiroSurge - Telemanipulation in Minimally Invasive Surgery". Retrieved April 2011, from http://www.dlr.de/rm/en/desktopdefault.aspx/tabid-3835/.

[23] van den Bedem, L. e. (2008). "Design of Slave Robot for Laparoscopic and Thoracoscopic Surgery". *20th International Conference of Society for Medical Innovation and Technology*. Vienna.

[24] Hannaford, B. e. (2009). "*Evaluation of RAVEN Surgical Telerobot during the NASA"*. Retrieved September 2010, from https://www.ee.washington.edu/techsite/papers/documents/.

[25] O. S. Bholat, R. S. Haluck, W. B. Murray, P. J. Gorman, and T. M. Krummel, "Tactile Feedback Is Present During Minimally Invaisve Surgery," Journal of American College of Surgeons, vol. 189, no. 4, pp. 349–355, 1999.

[26] D. Salle, P. Bidaud, and G. Morel, "Optimal Design of High Dexterity Modular MIS Instrument for Coronary Artery Bypass Grafting," in ICRA - Proc. of the IEEE Int. Conf. on Robotics and Automation, vol. 2, Apr. 2004, pp. 1276–1281, DOI: 10.1109/ROBOT.2004.1308000.

[27] J. Peirs, J. Clijnen, P. Herijgers, D. Reynaerts, H. V. Brussel, B. Corteville, and S. Boone, "Design of and Optical Force Sensor for Force Feedback during Minimally Invasive Robotic Surgery," in Eurosensors XVII, The 17th European conference on Solid-State Transducers, Guimaraes, Portugal, 2003.

[28] M. Kitagawa, "Indirect Feedback of Haptic Information for Robot-Assisted Telemanipulation," Master's thesis, Johns Hopkins University, Sep. 2003.

[29] L. Verner, K. Jeung, and A. Okamura, "The Effects of Gripping and Translational Forces on Teleoperation," in ICRA - Proc. of the IEEE Int. Conf. on Robotics and Automation, Workshop on Multi point Interaction in Robotics and Virtual Reality, 2004.

[30] E. Braun, C. Gaertner, H. Mayer, C. Staub, A. Knoll, R. Lange, and R. Bauernschmitt, "Features in Telemanipulation for Heart Surgery: Haptic Tasks," in World Congress on Medical Physics and Biomedical Engineering, ser. IFMBE Proceedings, O. D¨ossel and W. C. Schlegel, Eds., vol. 25/VI. Springer, Sep. 2009, pp. 6–7.

[31] I. Brouwer, J. Ustin, L. Bentley, A. Sherman, N. Dhruv, and F. Tendick, "Measuring In Vivo Animal Soft Tissue Properties for Haptic Modeling in Surgical Simulation," in MMVR - Annual Medicine Meets Virtual Reality Conference, J.W. et al., Ed. IOS Press, 2001.

[32] C. Wagner, N. Stylopoulos, and R. Howe, "The Role of Force Feedback in Surgery: Analysis of Blunt Dissection," in Proc. of the 10th Symposium on Haptic Interfaces for Virtual Environment and Teleoperator Systems (HAPTICS), Mar. 2002, pp. 68–74. [Online]. Available: http://biorobotics.harvard.edu/research/ff surgery.html

[33] J. Müller, "Charité, Klinik für Allgemein-, Visceral-, Gefäß- und Thoraxchirurgie, Campus Mitte," discussion, 2004.

[34] M. Kitagawa, D. Dokko, A. M. Okamura, B. T. Bethea, and D. D. Yuh, "Effect of Sensory Substitution on Suture Manipulation Forces for Surgical Teleoperation," in MMVR - Annual Medicine Meets Virtual Reality Conference, Newport Beach, CA, USA, Jan. 2004, submitted.

[35] M. E. Hagen, J. J. Meehan, I. Inan, and P. Morel, "Visual clues act as a substitute for haptic feedback in robotic surgery." Surgical Endoscopy, vol. 22, no. 6, pp. 1505 –1508, 2008.

[36] C. R. Wagner, "Force Feedback In Surgery: Physical Constraints and Haptic Information,"Ph.D. dissertation, Harvard University, Division Of Engineering and Applied Sciences, Cambridge, Massachusetts, USA, Jun. 2006.

[37] B. Deml, T. Ortmaier, and H. Weiss, "Minimally Invasive Surgery: Empirical Comparison of Manual and Robot Assisted Force Feedback Surgery," in Proc. of Euro-Haptics, Jun. 2004.

[38] C. R. Wagner and R. D. Howe, "Force Feedback Benefit Depends on Experience in Multiple Degree of Freedom Robotic Surgery Task," IEEE Transactions on Robotics, vol. 23, no. 6, pp. 1235–1240, Dec. 2007, DOI: 10.1109/TRO.2007.904891.

[39] M. Kitagawa, "Indirect Feedback of Haptic Information for Robot-Assisted Telemanipulation," Master's thesis, Johns Hopkins University, Sep. 2003.

[40] T. Akinbiyi, C. E. Reiley, S. Saha, D. Burschka, C. J. Hasser, D. D. Yuh, and A. M. Okamura, "Dynamic Augmented Reality for Sensory Substitution in Robot-Assisted Surgical Systems," in Proc. of the 28th IEEE EMBS Annual Int. Conf., New York City, NY, USA, Aug. 2006, pp. 567–570, DOI: 10.1109/IEMBS.2006.259707.

[41] S. Saha, "*Appropriate Degrees of Freedom of Force Sensing in Robot-Assisted Minimally Invasive Surgery*," Master's thesis, Johns Hopkins University, Baltimore, Maryland, USA, May 2005.

[42] J. Rosen, B. Hannaford, and R. Satava, "*Surgical Robotics: Systems Applications and Visions"*. (Springer Science & Business Media, 2011).

[43] D. Hu, Y. Gong, B. Hannaford, and E. J. Seibel. "*Semi-autonomous Simulated Brain Tumor Ablation with Raven II Surgical Robot using Behavior Tree*". In In-ternational Conference on Robotics and Automation, pp. 3868{3875, (2015). ISBN 9781479969234.61. B. Kehoe, G. Kahn, J. Mahler, J. Kim, A. Lee, A. Lee, K. Nakagawa, S. Patil, W. D.

[44] Boyd, P. Abbeel, and K. Goldberg. "*Autonomous Multilateral Debridement with the Raven Surgical Robot*". In International Conference on Robotics and Automation, pp. 1432{1439, (2014). ISBN 9781479936854.

[45] Marescaux J, Leroy J, Gagner M, et al: "Telesurgery". Nature 413:379-380, 2001.

[46] Fabrizio, M.D.; Lee, B.R.; Chan, D.Y.; Stoianovici, D.; Jarrett, T.W.; Yang, C. & Kavoussi, L.R. (2000). "*Effect of time delay on surgical performance during telesurgical manipulation*", *Journal of Endourology*, Vol. 14, No. 2, March 2000.

[47] Anvari, M. (2004)." *Robot-Assisted Remote Telepresence Surgery", Surgical Innovation*, Vol.,11,No., 2, pp.123-128.

[48] Pappone, C.; Vicedomini, G.; Manguso, F.; Gugliotta, F.; Mazzone, P.; Gulletta, S.; Sora, N.;Sala, S.; Marzi, A.; Augello, A.; Livolsi, L.; Santagostino, A. & Santinelli, V. (2006)."*Robotic Magnetic Navigation for Atrial Fibrillation Ablation", Journal of the AmericanCollege of Cardiology*, Vol., 47, No., 7, 2006, ISSN 0735-1097.

[49] Arata, Jumpei, Hiroki Takahashi, Phongsaen Pitakwatchara, Shin'ichi Warisawa, Kazuo Tanoue, Kozo Konishi, Satoshi Ieiri et al. "A remote surgery experiment between Japan and Thailand over Internet using a low latency CODEC system." In *Robotics and Automation, 2007 IEEE International Conference on*, pp. 953-959. IEEE, 2007.

[50] Smith, Roger, and Sanket Chauhan. "Using simulators to measure communication latency effects in robotic telesurgery." *Interservice/Industry Training, Simulation, and Education Conference (I/ITSEC) 2012*.

[51] Ainchwar, Arpit. "*Determination of Cycle Time Constraints in Case of Link Failure in Closed Loop Control in Internet of Things."* PhD diss., Université d'Ottawa/University of Ottawa, 2017.

[52] Rudolph Emil Kalman. "*A new approach to linear filtering and prediction problems*". *Transactions of the ASME–Journal of Basic Engineering*, 82(Series D):35–45, 1960.

[53] Huibert Kwakernaak and Raphael Sivan. "*Linear Optimal Control Systems"*. Wiley-Interscience, 1972a.

[54] Richard W. Freedman and Alok Bhatia. "A*daptive dynamic matrix control: Online evaluation of the dmc model coefficients". American Control Conference, 1985*, pages 220–225, 1985.

[55] Alberto Bemporad, Manfred Morari, Vivek Dua, and Efstratios N. Pistikopoulos. "*The explicit linear quadratic regulator for constrained systems"*. *Automatica*, 38:3–20, 2002. doi: 10.1016/S0005-1098(01)00174-1.

[56] J. Maciejowski. "*Predictive Control with Constraints"*. Tokyo Denki University Press, Prentice Hall, 2002.

[57] Huibert Kwakernaak and Raphael Sivan. "*Linear Optimal Control Systems"*. Wiley-Interscience, 1972a.

[58] J. Maciejowski. "*Predictive Control with Constraints"*. Tokyo Denki University Press, Prentice Hall, 2002.

[59] D. Q. Mayne, J.B. Rawling, C.V. Rao, and P. O. M. Scokaert. "*Constrained model predictive control: Stability and optimality"*. *Automatica*, 36:789–814, 2000. doi:10.1016/S0005-1098(99)00214-9.

[60] Lu, Mu-Chiao. "*Delay Identification and Model Predictive Control of Time Delayed Systems*." PhD diss., McGill University, 2008.

[61] E.F. Camacho and C. Bordons. "*Model Predictive Control*". Springer, 2003.

[62] D.Q. Mayne, J.B. Rawlings, C.V. Rao, and P.O.M. Scokaert." *Constrained model predictive control: statility and optimality*". Automatica, 36(6):789–814, 2000.

[63] J.L. Jerez, E.C. Kerrigan, and G.A. Constantinides. "*A condensed and sparse qp formulation for predictive control*". *Decision and Control and European Control Conference*, pages 5217–5222, 2010. doi: 10.1109/CDC.2011.6160293.

[64] M.V. Kothare, V. Balakrishnan, and M. Morari. "*Robust constrained model predictive control using linear matrix inequalities*". Automatica, 32(10):1361–1379, 1996.

[65] J.P. Richard. Time delay systems: "*an overview of some recent advances and open problems*". Automatica, 39(9):1667–1694, 2003.

[66] W.H. Kwon, J.W. Kang, Y.S. Lee, and Y.S. Moon. "*A simple receding horizon control for state delayed systems and its stability criterion"*. Journal of Process Control, 13:539–551, 2003.

[67] W.H. Kwon, Y.S. Lee, and S.H. Han. "*Receding horizon predictive control for linear time-delay systems*". SICE Annual Conference in Fukui, August 2003.

[68] W.H. Kwon, Y.S. Lee, and S.H. Han. "*General receding horizon control for linear time-delay systems*". Automatica, 40:1603–1611, 2004.

[69] Mathworks (2018, 20 May) Retrived from https://www.mathworks.com/help/mpc/ug/optimization-problem.html

[70] S.C. Jeong and P.G. Park. Constrained mpc algorithm for uncertain timevarying systems with state-delay. IEEE transactions on Automatic Control, 50(2):257–263, 2005.

[71] X.B. Hu and W.H. Chen. Model predictive control for constrained systems with uncertain state-delays. International Journal of Robust and Nonlinear Control, 14:1421–1432, 2004.

[72] W.H. Kwon, S.H. Han, and Y.S. Lee. Receding-horizon predictive control for nonlinear time-delay systems with and without input constraints. IFAC symposium on dynamics and control of process systems, pages 277–282, June 2001.

[73] S. Oblak and I. Skrjanc. Continuous-time nonlinear model predictive control of time-delayed wiener-type systems. Proceeding of the 25th IASTED International Conference Modelling, Idenfication, and Control, pages 1–6, February 2006. Lanzarote, Canary Islands, Spain.

[74] C.L. Su and S.Q. Wang. Robust model predictive control for discrete uncertain nonlinear system with time-delay via fuzzy model. Journal of Zhejiang University Science A, 7(10):1723–1732, 2006.

[75] D.L. Yu and J.B. Gomm. Implementation of neural network predictive control to a multivariable chemical reactor. Control Engineering Practice, 11:1315–1323, 2003.

[76] D. Richert and C. Macnab, \Direct Adaptive Force Feedback for Haptic Control with Time Delay," in IEEE Toronto International Conference Science and Technology for Humanity (TIC-STH). IEEE, Sept. 2009, pp. 893-897.

[77] Ortmaier, Tobias. "Motion compensation in minimally invasive robotic surgery." PhD diss., Technische Universität München, 2003.

[78] N. Chopra, P. Berestesky and M.W. Spong. Bilateral teleoperation over unreliable communication networks. IEEE Transactions on Control Systems Technology, vol. 16, no. 2, pages 304–313, 2008.

[79] A. Kruszewski, W.-J. Jiang, E. Fridman, J.-P. Richard and A. Toguyeni. A switched system approach to exponential stabilization through communication network. IEEE Transactions on Control Systems Technology, to appear, 2011.

[80] J.-P. Richard. Time delay systems: an overview of some recent advances and open problems. Automatica, vol. 39, no. 10, pages 1667–1694, 2003.

[81] Z.H. Khan. Wireless network architecture for long range teleoperation of an autonomous system. PhD thesis, Universite de Grenoble, 2010.

[82] J.P. Hespanha, P. Naghshtabrizi and Y. Xu. A survey of recent results in networked control systems. Proceedings of the IEEE, vol. 95, no. 1, pages 138–162,2007.

[83] Handorf, Andrew M., and Wan-Ju Li. "Induction of mesenchymal stem cell chondrogenesis through sequential administration of growth factors within specific temporal windows." *Journal of cellular physiology* 229, no. 2 (2014): 162-171.

[84] Whitney and Nevins, 1979 Whitney, D. E. and Nevins, J. L. (1979).What is the remote center compliance (rcc) and what can it do ? In *Proc. of the Int. Symp. on Industrial Robots*, pages 135 152, Washington, USA.

[85] Salisbury, 1980 Salisbury, J. K. (1980). Active stiffness control of a manipulator in cartesian coordinates. In *Proc. of the IEEE Int. Conf.on Decision and Control*, pages 95–100, Albuquerque, Etats-Unis.

[86] Hogan, 1985 Hogan, N. (1985). Impedance control - an approach to manipulation. i - theory. ii implementation. iii - applications. *Trans.of the ASME, J. of Dynamic Systems, Measurement, and Control*,107:1–24.

[87] Lawrence, 1988 Lawrence, D. A. (1988). Impedance control stability properties in common implementations. In *Proc. of the IEEE Int.Conf. on Robotics and Automation*, pages 1185–1190, Philadelphia,USA.

[88] Dominici, Michel, and Rui Cortesao. "Model predictive control architectures with force feedback for robotic-assisted beating heart surgery." In *Robotics and Automation (ICRA), 2014 IEEE International Conference on*, pp. 2276-2282. IEEE, 2014.

[89] Rocco, Paolo, Gianni Ferretti, and Gianantonio Magnani. 1997. "Implicit Force Control for Industrial Robots in Contact with Stiff Surfaces." *Automatica* 33 (11): 2041-2047. doi:10.1016/S0005-1098(97)00113-1.

[90] Lu, M. C. (2008). Delay Identification and Model Predictive Control of Time Delayed Systems (Doctoral dissertation, McGill University).

Appendix

Base Code for the force control, kinematic Predictive imaging, and Minimum impact in

MATLAB

//

```
Jm1=5.e-3;
Jm2=2.e-3;

Kel1=70;
Kel2=70;
Kel=diag([Kel1,Kel2]);

Del1=0.05;
Del2=0.05;

%Reduction ratios
n1=100;
n2=100;
N=diag([n1,n2]);


L1 = Link('d', 0, 'a', 1, 'alpha', 0);
L1.m=50;
L1.r=[-0.5,0,0];
L1.I=[0,0,0;0,0,0;0,0,10];
L1.G=1;
L1.Jm=0;

%Note:  motors and transmissions are defined outside the
block which simulates the robot

L2=Link(L1);
L2.G=1;
L2.Jm=0;

r2=SerialLink([L1,L2]);

r2.name='Robodoc';
```

```
r2.gravity=[0,9.81,0];

Ke=5.e+5;

ye=-2.82e-5;

Fd=10;

n=[0;-1];

t0=1.5;

T=15;

sd1=0.01;

h=0.03;


ta=(T*sd1-h)/sd1;

amax=sd1/ta;

s0=0.2;

qrif0=r2.ikine([eye(3),[0.2;0;0];[0,0,0,1]],[-1,3],[1 1 0 0
0 0 ]);

qm0=qrif0*N;

q0=fsolve(@(q0) N*Kel*(qm0'-N*q0')-

r2.gravload(q0)'+r2.jacob0(q0)'*[n;0;0;0;0]*Fd,qrif0);

tau0=r2.gravload(q0)'-r2.jacob0(q0)'*[n;0;0;0;0]*Fd;

taum0=inv(N)*tau0;

Jl1=60;
Jl2=22.5;

Jlr1=Jl1/n1^2;
Jlr2=Jl2/n2^2;

%Inertia ratios
```

```
ro1=Jlr1/Jm1;
ro2=Jlr2/Jm2;


mu1=1/(Jm1+Jlr1);
wz1=sqrt(Kel1/Jlr1);
csiz1=0.5*Del1/sqrt(Jlr1*Kel1);
wp1=sqrt(1+ro1)*wz1;
csip1=sqrt(1+ro1)*csiz1;
Gvm1=tf(mu1*[1/wz1^2 2*csiz1/wz1 1],[1/wp1^2 2*csip1/wp1 1
0]);


Tiv1=10/wz1;
Kiv1=10.4; %Da rltool
Kpv1=Kiv1*Tiv1;
wcv1=Kpv1*mu1;
wtildecv1=wcv1/wz1;

Rv1 = tf([Kpv1 Kiv1],[1 0]);
Lv1=Gvm1*Rv1;
Fv1=feedback(Lv1,1);
Gpm1 = Fv1*tf(1,[1 0]);
Kpp1=28.7; %From rltool

%Parameters: axis 2

mu2=1/(Jm2+Jlr2);
wz2=sqrt(Kel2/Jlr2);
csiz2=0.5*Del2/sqrt(Jlr2*Kel2);
wp2=sqrt(1+ro2)*wz2;
csip2=sqrt(1+ro2)*csiz2;
Gvm2=tf(mu2*[1/wz2^2 2*csiz2/wz2 1],[1/wp2^2 2*csip2/wp2 1
0]);

%Tuning: axis 2 controller

Tiv2=10/wz2;
Kiv2=10.4; %Da rltool
Kpv2=Kiv2*Tiv2;
wcv2=Kpv2*mu2;
wtildecv2=wcv2/wz2;

Rv2 = tf([Kpv2 Kiv2],[1 0]);
```

```
Lv2=Gvm2*Rv2;
Fv2=feedback(Lv2,1);
Gpm2 = Fv2*tf(1,[1 0]);
Kpp2=45;


KP1=n1^2*Kpv1*(Kpp1+1/Tiv1);
KD1=n1^2*Kpv1;
KI1=n1^2*Kpp1*Kpv1/Tiv1;

KP2=n2^2*Kpv2*(Kpp2+1/Tiv2);
KD2=n2^2*Kpv2;
KI2=n2^2*Kpp2*Kpv2/Tiv2;

KPF=-20;
KIF=-80;

for ct = 1:1:10

 t01(ct,:)=1.3 + (ct-1)*0.02;
 %Travel time

 T1=15 ;

sd1=0.01;

h1=0.03;

 s0=0.2;
 ta1(:)=(T1*sd1-h1)/sd1;
 amax1=sd1/ta1(:);
end
```